On the production and transfer of entangled electrons and photons

Velsen, J. van

On the production and transfer of entangled electrons and photons

Joris van Velsen

On the production and transfer of entangled electrons and photons

PROEFSCHRIFT

ter verkrijging van
de graad van Doctor aan de Universiteit Leiden,
op gezag van de Rector Magnificus Dr. D. D. Breimer,
hoogleraar in de faculteit der Wiskunde en
Natuurwetenschappen en die der Geneeskunde,
volgens besluit van het College voor Promoties
te verdedigen op woensdag 28 september 2005
te klokke 15.15 uur

door

Joris Lodewijk van Velsen

geboren te Wageningen op 27 juli 1977

Promotiecommissie:

Promotor:	Prof. dr. C. W. J. Beenakker
Referent:	Prof. dr. J. P. Woerdman
Overige leden:	Prof. dr. P. H. Kes
	Prof. dr. G. Nienhuis
	dr. L. M. K. Vandersypen

Het onderzoek beschreven in dit proefschrift is onderdeel van het wetenschappelijke programma van de Stichting voor Fundamenteel Onderzoek der Materie (FOM) en de Nederlandse Organisatie voor Wetenschappelijk Onderzoek (NWO).

The research described in this thesis has been carried out as part of the scientific programme of the Foundation for Fundamental Research on Matter (FOM) and the Netherlands Organisation for Scientific Research (NWO).

Aan mijn ouders

Contents

Chapter 1

Introduction

The nonclassical correlation known as entanglement is one of the most counter-intuitive features of quantum mechanics and plays a central role in the emerging field of quantum computing and quantum information processing [1]. Two spatially separated particles are entangled if their joint state can not be prepared by operating on each particle separately — not even with the exchange of classical bits of information.

Entanglement is called a "resource" because it is both precious and useful: It is *precious*, because if the quantum correlation is lost after the particles have been separated, it can not be restored without bringing them back together. It is *useful*, because entangled pairs of particles enable the disembodied transfer (= teleportation) of quantum bits of information (= qubits), which is a basic step in quantum algorithms.

The two separate aspects of entanglement production and transfer studied in this thesis were motivated by two separate lines of experimental research. For the entanglement *transfer*, we were motivated by an experiment in Leiden on the transmission of entangled photons through strongly scattering metal plates [2]. We have developed a general scattering theory of entanglement transfer that accounts for the highly entangled transmitted photons in the experiment.

For the entanglement *production*, our motivation came from experiments in progress in Delft to produce and detect entangled electrons trapped in quantum dots [3]. These experiments require control over the electron-electron interactions on short distances, first to entangle the electrons and then to spatially separate them. As described in this thesis, we came up with an alternative scheme for entanglement production and detection with *free* electrons, that does not rely on electron-electron interactions.

The present chapter contains some background material on entanglement in general, and specifically on entanglement of electrons and photons.

1.1 Entanglement

The elementary entangled state is the spin singlet

$$|\Psi_{\text{Bell}}\rangle = \frac{1}{\sqrt{2}}\big(|\uparrow\rangle_A|\downarrow\rangle_B - |\downarrow\rangle_A|\uparrow\rangle_B\big), \tag{1.1}$$

also known as a Bell state. The indices A, B label two spatially separated particles and the arrows $\uparrow$, $\downarrow$ indicate two spin states. The Bell state (1.1) can not be created by local operations and classical communication, because it is not known, not even in principle, which particle carries which spin. This is in contrast to the nonentangled mixed state with density matrix

$$\rho_{\text{mixed}} = \frac{1}{2}\big(|\uparrow\rangle\langle\uparrow|\big)_A \otimes \big(|\downarrow\rangle\langle\downarrow|\big)_B + \frac{1}{2}\big(|\downarrow\rangle\langle\downarrow|\big)_A \otimes \big(|\uparrow\rangle\langle\uparrow|\big)_B. \tag{1.2}$$

The state ρ_{mixed} can be created by tossing with a coin: heads means A is $\uparrow$ and B is $\downarrow$, while tails means A is $\downarrow$ and B is $\uparrow$. By exchanging classical bits (heads or tails) and then locally rotating the spin, an ensemble described by ρ_{mixed} is prepared.

1.1.1 Bell inequality

The spins in the state $|\Psi_{\text{Bell}}\rangle$ are correlated; a measurement of one spin, say with outcome $\uparrow$, projects the other spin on the opposite spin state $\downarrow$. The same applies to ρ_{mixed}. The difference between the correlation of the pure entangled state (1.1) and the correlation of the mixed nonentangled state (1.2) is that the former persists if we measure the spin along a different axis, while the latter is diminished. For example, the change of basis

$$|\uparrow\rangle \to \frac{1}{\sqrt{2}}\big(|\uparrow\rangle + |\downarrow\rangle\big), \quad |\downarrow\rangle \to \frac{1}{\sqrt{2}}\big(|\uparrow\rangle - |\downarrow\rangle\big) \tag{1.3}$$

(both for spin A and spin B) leaves $|\Psi_{\text{Bell}}\rangle$ invariant, but ρ_{mixed} becomes a mixture of parallel and anti-parallel spins.

The perfect anti-correlation of the entangled state (1.1) along any direction was referred to by Einstein, Podolsky, and Rosen (EPR) as "spooky action at a distance" [4]. There is, however, no conflict with causality: If a measurement is

performed on one particle, no information concerning the definite outcome of an experiment is transmitted to the other particle without classical communication on the choice of spin direction and the measurement result.

The correlations of nonentangled states can be described by classical mechanics in terms of the local and realistic theory (LRT) of EPR [4]. The correlation of the entangled state (1.1), however, goes beyond the LRT. This was demonstrated by Bell [5], who derived an inequality which is satisfied by the classical correlations of nonentangled states, but can be violated by the quantum correlations of entangled states.

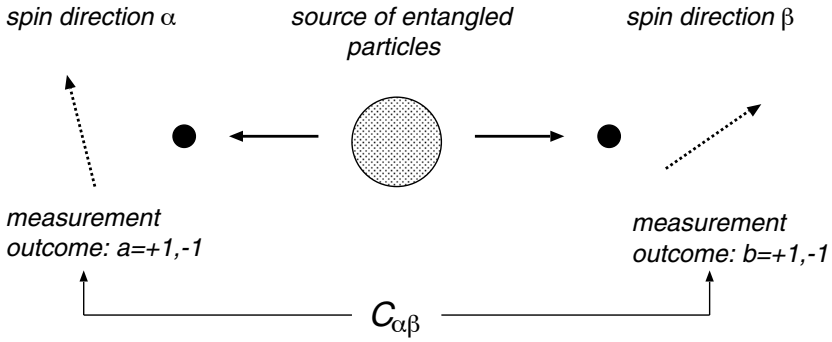

Figure 1.1: Scheme to detect entanglement by violation of the Bell inequality.

To explain the Bell inequality, we consider the setup indicated in Fig. 1.1. It consists of a source producing a pair of particles in the Bell state. Two local observers A and B each have a particle at their disposal. Within the LRT, measurement results can not depend on the choice of measurement of another spatially separated observer (locality) and the results of any measurement are predetermined, regardless of whether the measurement is carried out or not (realism). Observers A and B each measure their spin along directions $\boldsymbol{\alpha}$ and $\boldsymbol{\beta}$ with outcome $a = \pm 1$ and $b = \pm 1$, respectively. The correlator of the LRT is

$$C_{\boldsymbol{\alpha\beta}} = \sum_{\lambda} p(\lambda) a(\boldsymbol{\alpha}, \lambda) b(\boldsymbol{\beta}, \lambda). \tag{1.4}$$

The "hidden" variable λ, with probability $p(\lambda)$ in the ensemble, predetermines the measurement outcomes. By averaging the identity

$$a(\boldsymbol{\alpha}, \lambda) b(\boldsymbol{\beta}, \lambda) + a(\boldsymbol{\alpha}, \lambda) b(\boldsymbol{\beta'}, \lambda) + a(\boldsymbol{\alpha'}, \lambda) b(\boldsymbol{\beta}, \lambda) - a(\boldsymbol{\alpha'}, \lambda) b(\boldsymbol{\beta'}, \lambda) \equiv \pm 2 \tag{1.5}$$

over the ensemble of hidden variables, one obtains for the LRT the Clauser-Horne-Shimony-Holt (CHSH) form of the Bell inequality [6],

$$\mathcal{E} = \left| C_{\boldsymbol{\alpha\beta}} + C_{\boldsymbol{\alpha\beta'}} + C_{\boldsymbol{\alpha'\beta}} - C_{\boldsymbol{\alpha'\beta'}} \right| \leq 2. \tag{1.6}$$

In quantum mechanics the correlator $C_{\boldsymbol{\alpha\beta}}$ is given, instead of by Eq. (1.4), by the expectation value

$$C_{\boldsymbol{\alpha\beta}} = \langle (\boldsymbol{\alpha}\cdot\boldsymbol{\sigma})_A \otimes (\boldsymbol{\beta}\cdot\boldsymbol{\sigma})_B \rangle. \tag{1.7}$$

Here $\boldsymbol{\sigma} = (\sigma_x, \sigma_y, \sigma_z)$ is the vector of Pauli matrices

$$\sigma_x = \begin{pmatrix} 0 & 1 \\ 1 & 0 \end{pmatrix}, \quad \sigma_y = \begin{pmatrix} 0 & -i \\ i & 0 \end{pmatrix}, \quad \sigma_z = \begin{pmatrix} 1 & 0 \\ 0 & -1 \end{pmatrix}. \tag{1.8}$$

If Eq. (1.7) is inserted into Eq. (1.6) one finds that this inequality can be violated for certain states. These states can therefore not be described by the LRT, but must be described quantum mechanically.

All nonentangled states obey the Bell-CHSH inequality. If $\mathcal{E} > 2$ for some choice of unit vectors $\boldsymbol{\alpha}$, $\boldsymbol{\alpha'}$, $\boldsymbol{\beta}$, $\boldsymbol{\beta'}$, then the spins are entangled. The converse of this statement is not true: There exist mixed states that are entangled and satisfy $\mathcal{E} \leq 2$ for all sets of unit vectors (see Sec. 1.1.3). The pure Bell state (1.1) has correlator $C_{\boldsymbol{\alpha\beta}} = -\boldsymbol{\alpha}\cdot\boldsymbol{\beta}$ and allows for the largest possible violation $\mathcal{E} = 2\sqrt{2} > 2$ of the Bell-CHSH inequality.

1.1.2 Entanglement measures for pure states

An arbitrary pure state $|\Psi\rangle$ in the bipartite Hilbert space $\mathcal{H} = \mathcal{H}_A \otimes \mathcal{H}_B$ of a pair of two-level systems (= qubits) takes the form

$$|\Psi\rangle = \sum_{i=1}^{2}\sum_{j=1}^{2} c_{ij}\,|i\rangle_A |j\rangle_B, \quad \mathrm{Tr}\, c^\dagger c = 1. \tag{1.9}$$

The basis states $|1\rangle$, $|2\rangle$ may refer to spins (electrons), polarizations (photons), or other degrees of freedom.

Since an entangled state can not be prepared locally, one needs to exchange a certain amount of quantum information to create it out of a product state. This quantum information can take the form of Bell pairs (1.1), shared between A and B. Bell pairs play the role of a "currency", by means of which one can quantify entanglement. The average number of Bell pairs per copy needed to prepare a large number of copies of the pure state $|\Psi\rangle$ is given by [7]

$$E = -\mathrm{Tr}_A \rho_A \log_2 \rho_A, \quad \rho_A = \mathrm{Tr}_B |\Psi\rangle\langle\Psi|. \tag{1.10}$$

(The reduced density matrix ρ_A of subsystem A is obtained by tracing out the degrees of freedom of subsystem B.)

The quantity $E \in [0,1]$ is called the entanglement entropy, or entanglement of formation. In terms of the 2×2 matrix of coefficients c, it takes the form

$$E = \mathcal{F}\Big(\frac{1}{2} + \frac{1}{2}\sqrt{1 - 4\,\mathrm{Det}\, c^\dagger c}\Big), \tag{1.11}$$

where the function $\mathcal{F}(x)$ is defined by

$$\mathcal{F}(x) = -x \log_2 x - (1-x)\log_2(1-x). \tag{1.12}$$

The concurrence $\mathcal{C} \in [0,1]$ is in one-to-one relation with E but has a somewhat simpler expression:

$$\mathcal{C} = 2\sqrt{\mathrm{Det}\, c^\dagger c}. \tag{1.13}$$

A Bell pair has unit concurrence and entanglement of formation, while both $\mathcal{C}$ and E vanish for a product state.

For a pure state, the degree by which the Bell-CHSH inequality can be violated is in one-to-one relation to the concurrence $\mathcal{C}$. By maximizing the correlator

$$\mathcal{E}_{\max} = \max_{\alpha,\beta,\alpha',\beta'} \big| C_{\alpha\beta} + C_{\alpha\beta'} + C_{\alpha'\beta} - C_{\alpha'\beta'} \big| \tag{1.14}$$

over four unit vectors, one obtains the Bell-CHSH parameter $\mathcal{E}_{\max}$. The relation between $\mathcal{E}_{\max}$ and $\mathcal{C}$ is [8]

$$\mathcal{E}_{\max} = 2\sqrt{1 + \mathcal{C}^2}. \tag{1.15}$$

The Bell-CHSH parameter $\mathcal{E}_{\max}$ ranges from 2 to $2\sqrt{2}$ as the concurrence ranges from 0 to 1.

1.1.3 Entanglement measures for mixed states

The density matrix ρ of a mixed state can be decomposed into pure states $|\Psi_n\rangle$ with positive weight p_n,

$$\rho = \sum_n p_n |\Psi_n\rangle\langle\Psi_n|, \quad p_n > 0, \quad \sum_n p_n = 1. \tag{1.16}$$

The states $|\Psi_n\rangle$ are normalized to unity, $\langle\Psi_n|\Psi_n\rangle = 1$, but they need not be orthogonal. The convex-sum decomposition is therefore not unique — there are many equivalent representations of ρ as a mixture of pure states.

A mixed state in the bipartite Hilbert space $\mathcal{H}_A \otimes \mathcal{H}_B$ is nonentangled (= separable) if there exists a convex-sum decomposition into pure product states,

meaning that $|\Psi_n\rangle = |\Phi_n\rangle_A |\Phi'_n\rangle_B$ with $|\Phi_n\rangle \in \mathcal{H}_A$ and $|\Phi'_n\rangle \in \mathcal{H}_B$ for all n. The entanglement entropy E of a separable mixed state vanishes, with the definition [9]

$$E = \min_{\{\Psi_n, p_n\}} \sum_n p_n E(\Psi_n). \tag{1.17}$$

Here $E(\Psi_n)$ is the entanglement entropy of the pure state $|\Psi_n\rangle$, defined in Eq. (1.10), and the minimum is taken over all convex-sum decompositions of ρ. The entanglement of formation E has a closed form expression given by [10]

$$E = \mathcal{F}\left(\frac{1}{2} + \frac{1}{2}\sqrt{1-\mathcal{C}^2}\right), \tag{1.18}$$

$$\mathcal{C} = \max\left(0, \sqrt{\lambda_1} - \sqrt{\lambda_2} - \sqrt{\lambda_3} - \sqrt{\lambda_4}\right). \tag{1.19}$$

The λ_i's are the eigenvalues of the matrix product $\rho(\sigma_y \otimes \sigma_y)\rho^*(\sigma_y \otimes \sigma_y)$, in the order $\lambda_1 \geq \lambda_2 \geq \lambda_3 \geq \lambda_4$. The quantity $\mathcal{C}$ is again called the concurrence. For a pure state (with $\rho^2 = \rho$) the definition (1.19) of $\mathcal{C}$ is equivalent to Eq. (1.13).

The Bell-CHSH parameter $\mathcal{E}_{\max}$ for an arbitrary mixed state of two qubits was analyzed in Refs. [11, 12]. Unlike for a pure state, for a mixed state there is no one-to-one relation between $\mathcal{C}$ and $\mathcal{E}_{\max}$. Depending on the density matrix, $\mathcal{E}_{\max}$ can take on values between $2\mathcal{C}\sqrt{2}$ and $2\sqrt{1+\mathcal{C}^2}$. The dependence of $\mathcal{E}_{\max}$ on ρ involves the two largest eigenvalues u_1 and u_2 of the real symmetric 3×3 matrix $R^{\mathrm{T}}R$ constructed from $R_{kl} = \mathrm{Tr}\rho\,\sigma_k \otimes \sigma_l$, where $\sigma_1 = \sigma_x$, $\sigma_2 = \sigma_y$, and $\sigma_3 = \sigma_z$. The relation is

$$\mathcal{E}_{\max} = 2\sqrt{u_1 + u_2}. \tag{1.20}$$

Violation of the Bell-CHSH inequality ($\mathcal{E}_{\max} > 2$) implies $\mathcal{C} > 0$, but not the other way around. That is, there exist entangled mixed states ($\mathcal{C} > 0$) that can not violate the Bell-CHSH inequality ($\mathcal{E}_{\max} \leq 2$).

1.2 How to entangle photons

To produce entangled photons one can distinguish methods which rely on interactions between the photons (nonlinear optics) and methods which do not need interactions (linear optics).

1.2.1 Nonlinear optics

The production of polarization-entangled photons by means of interactions uses a nonlinear crystal effect known as parametric down-conversion [13]. The scheme

is indicated schematically in Fig. 1.2. A single pump photon of frequency 2ω is converted into two photons of frequency ω in different cones of orthogonal polarizations H and V. By collecting photons only along the two intersections of the cones, it is not known, not even in principle, which photon carries which polarization. This corresponds to the maximally entangled two-photon state

$$|\Psi\rangle = \frac{1}{\sqrt{2}}\left(|\mathrm{H}\rangle_A|\mathrm{V}\rangle_B + e^{i\phi}|\mathrm{V}\rangle_A|\mathrm{H}\rangle_B\right). \tag{1.21}$$

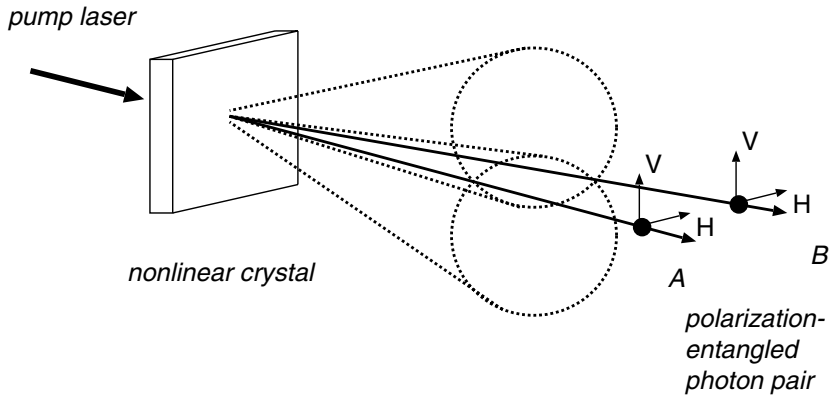

Figure 1.2: Scheme to create polarization-entangled photons by means of parametric down-conversion.

1.2.2 Linear optics

A linear optical way of entangling photons is by means of elastic scattering at a beam splitter, see Fig. 1.3. A necessary condition for entanglement by linear optics is the nonclassicality of the photon sources: If the photons are incident in photon number (Fock) states or squeezed states, their polarizations can be entangled by a beam splitter [14]. However, classical states (such as thermal states or coherent states) can not be entangled. For a proof of this "no-go theorem", we follow Ref. [15].

The density matrix ρ_{in} of a multi-mode state incident from the sources onto

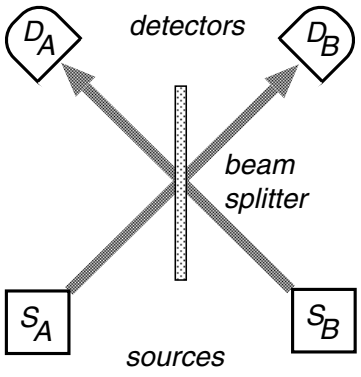

Figure 1.3: Scheme of entanglement production by a beam splitter.

the beam splitter can be written in the coherent state representation

$$\rho_{\rm in} = \int d\boldsymbol{\alpha}\, P(\boldsymbol{\alpha}) |\boldsymbol{\alpha}\rangle\langle\boldsymbol{\alpha}|, \quad |\boldsymbol{\alpha}\rangle = e^{\boldsymbol{a}^\dagger\cdot\boldsymbol{\alpha}-\boldsymbol{a}\cdot\boldsymbol{\alpha}^*}|0\rangle. \tag{1.22}$$

The coherent state $|\boldsymbol{\alpha}\rangle = |\alpha_1,\alpha_2,\ldots\rangle$ is an eigenstate of the annihilation operator a_n with complex eigenvalue α_n. (The mode index n labels frequencies and polarizations of modes to the left and the right of the beam splitter.) We have abbreviated $d\boldsymbol{\alpha} = \prod_n d{\rm Re}\,\alpha_n d{\rm Im}\,\alpha_n$. The real function $P(\boldsymbol{\alpha})$ may take on negative values. In that case the state $\rho_{\rm in}$ is called nonclassical, because $P(\boldsymbol{\alpha})$ can not be interpreted as a classical distribution. A thermal state is a classical state with a Gaussian $P(\boldsymbol{\alpha}) \propto \exp(-\sum_n |\alpha_n|^2/f_n)$, where f_n is the Bose-Einstein distribution.

The beam splitter transforms the annihilation operators $\boldsymbol{a} = \{a_1,a_2,\ldots\}$ of the incoming state into annihilation operators $\boldsymbol{b} = \{b_1,b_2,\ldots\}$ of the outgoing state. This is a unitary transformation,

$$b_n = \sum_m S_{nm} a_m, \quad SS^\dagger = \mathbb{1}, \tag{1.23}$$

defined by the scattering matrix S. The density matrix $\rho_{\rm out}$ of the outgoing state is obtained from $\rho_{\rm in}$ with the help of Eq. (1.23). The result is

$$\rho_{\rm out} = \int d\boldsymbol{\beta}\, P(S^\dagger\boldsymbol{\beta}) |\boldsymbol{\beta}\rangle\langle\boldsymbol{\beta}|, \quad |\boldsymbol{\beta}\rangle = e^{\boldsymbol{b}^\dagger\cdot\boldsymbol{\beta}-\boldsymbol{b}\cdot\boldsymbol{\beta}^*}|0\rangle. \tag{1.24}$$

We have made a change of variables from $\boldsymbol{\alpha}$ to $\boldsymbol{\beta} = S\boldsymbol{\alpha}$ and used that $d\boldsymbol{\alpha} = d\boldsymbol{\beta}$ because of the unitarity of S. The outgoing modes can be grouped into modes that

are detected by A and modes detected by B. Since the creation and annihilation operators of different modes commute, the pure state $|\boldsymbol{\beta}\rangle$ is separable. It follows that ρ_{out} is separable if $P \geq 0$ for any $\boldsymbol{\beta}$, because in that case the density matrix has a decomposition into separable pure states with positive weights. Nonclassicality is therefore a necessary condition for entangling photons at a beam splitter.

Even if we start from a nonclassical state, such as a two-photon Fock state, it is not garanteed that the beam splitter will produce entanglement. If, for instance, the two single photons are incident in wavepackets that are not timed to "collide" at the beam splitter, then their polarizations do not get entangled. This is because the photons are distinguishable by their temporal degrees of freedom.

1.3 How to entangle electrons

1.3.1 Interacting particles

Whereas violation of the Bell inequality has been demonstrated with photons [16], a similar achievement is still missing for electrons in the solid state. This may seem surprising, since entanglement in the solid state is the rule rather than the exception. The essential problem, however, lies in the controllable and coherent extraction of an entangled pair of electrons into two spatially separated conductors.

There have been a number of theoretical proposals for solid-state entanglers. These schemes rely on interactions, such as the Coulomb interaction in a quantum dot [17–20] or the pairing interaction in a superconductor [21–23]. Two examples of these proposals are indicated schematically in Fig. 1.4.

1.3.2 Free particles

In this thesis, we propose an entangler for free electron-hole excitations, where both entanglement generation as well as spatial separation are realized purely by elastic scattering. The proposal in its simplest form consists of a single-channel conductor separated in two regions by a tunnel barrier. Incoming states to the right of the barrier are filled up to the Fermi energy E_{F}, while the states to the left are filled up to $E_{\text{F}} + eV$ (see Fig. 1.5). Tunneling of an electron across the barrier produces an entangled electron-hole excitation $|\Psi\rangle$. If the tunneling is spin-independent, the spins of electron and hole are maximally entangled in the state

$$|\Psi\rangle = \frac{1}{\sqrt{2}}\big(|\uparrow\rangle_e|\uparrow\rangle_h + |\downarrow\rangle_e|\downarrow\rangle_h\big). \tag{1.25}$$

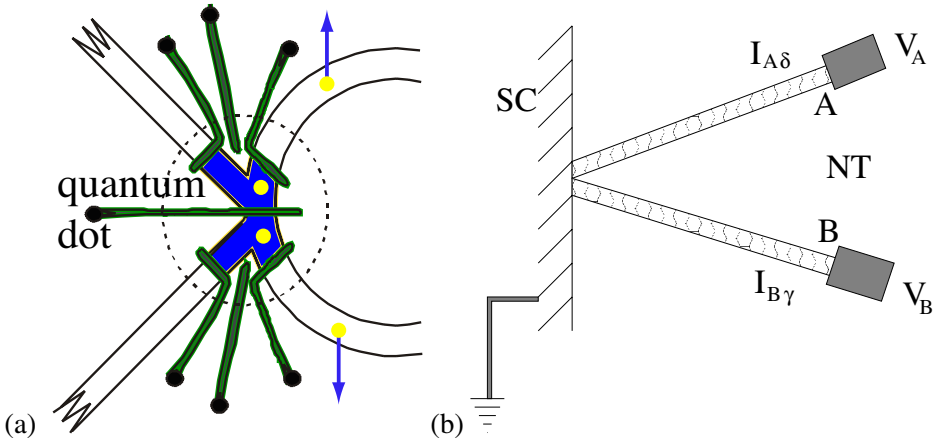

Figure 1.4: Solid-state entanglers making use of interactions. (a) Two coupled quantum dots with a single excess electron in each dot. The electron-pair is in its ground state, the entangled spin singlet state $|\Psi_{\text{Bell}}\rangle$. Spatial separation is due to strong on-site Coulomb repulsion (like in a hydrogen molecule). Mobile spin-entangled electrons are created by simultaneously lowering the tunnel barriers coupling each dot to separate leads. Picture by L. P. Kouwenhoven. (b) Two nanotubes (NT) are connected to a superconductor (SC). Each nanotube extracts an electron from a Cooper pair, generating spin-entangled currents $I_{A\delta}$ ($\delta = \uparrow, \downarrow$) and $I_{B\gamma}$ ($\gamma = \uparrow, \downarrow$) in the separate tubes A and B, respectively. Picture taken from Ref. [23].

Electron-hole pairs are entangled even if the electron reservoirs are in thermal equilibrium at temperature $kT \ll eV$. This is in contrast to the linear optics entanglement by a beam splitter, which does not work if the sources are in thermal equilibrium. The Fermi sea, while being in local equilibrium, works around the optical no-go theorem described in Sec. 1.2.2.

The creation of entangled electron-hole pairs has similarities and differences with respect to both the creation of entangled photons by a nonlinear crystal and at a beam splitter. On the one hand, a Bell pair is produced spontaneously, without requiring synchronization at the source, by the voltage applied over the tunnel barrier and by the laser beam incident on the nonlinear crystal, while the beam splitter requires two synchronized single-photon sources. On the other hand, the tunnel barrier and the beam splitter both do not require interactions between the particles, while the nonlinear crystal requires photon-photon interactions to split the pump photon into two photons of lower frequency. The electron-hole entan-

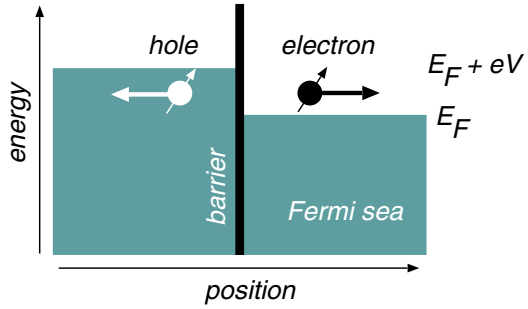

Figure 1.5: Schematic drawing of the electron-hole entangler proposed in this thesis. Tunneling events give rise to nonlocal spin correlations that can violate the Bell inequality.

gler and the optical entanglers are compared schematically in Fig. 1.6.

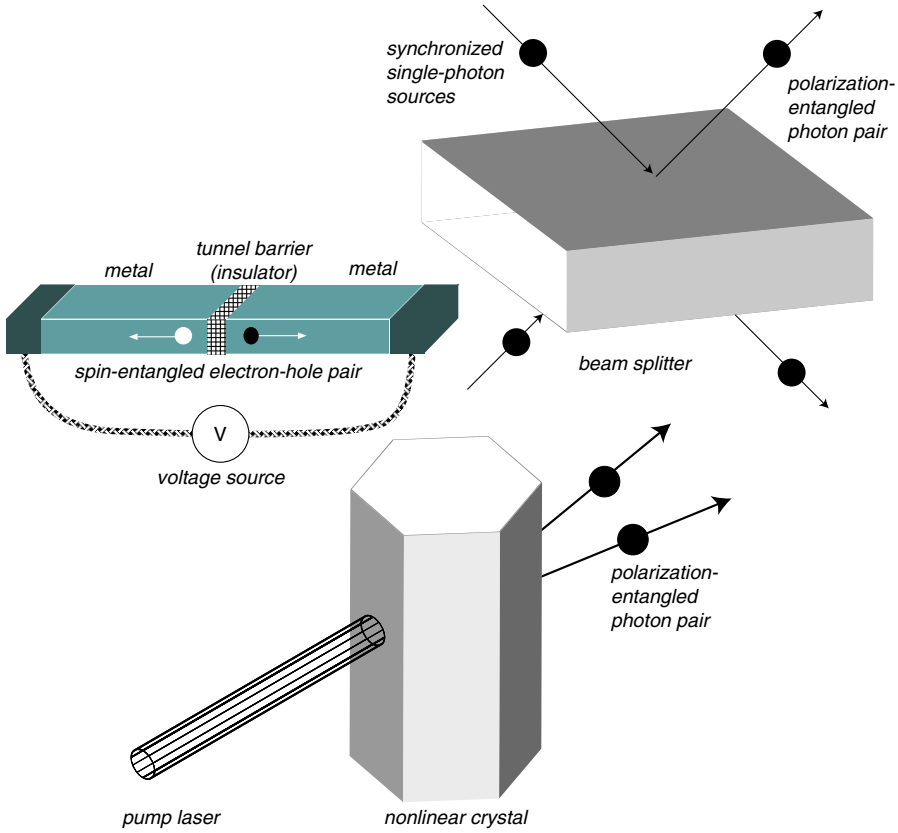

Figure 1.6: Schematic illustration of the entanglement of electron-hole pairs by a tunnel barrier and of photons by a nonlinear crystal and a beam splitter.

1.4 This thesis

Chapter 2: Production and detection of entangled electron-hole pairs in a degenerate electron gas

The chapters 2 and 3 deal with electrons. In chapter 2 we describe the electron-hole entangler of Sec. 1.3.2 and demonstrate that the spin currents carried by electron-hole pairs produced at a tunnel barrier violate a Bell inequality. To avoid the need for spin-resolved detection, we give an alternative implementation using edge channels in the quantum Hall effect. Many different implementations have been proposed following our initial proposal [24]. Some of these are indicated

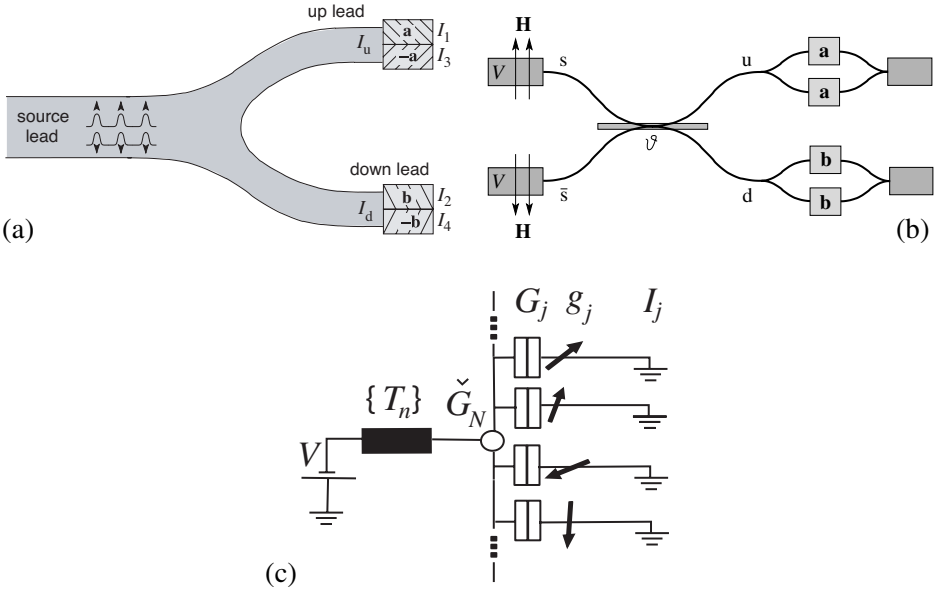

Figure 1.7: Three geometries to produce and detect spin-entanglement in a normal conductor with ferromagnetic contacts. Panels a, b, and c are taken, respectively, from Refs. [25], [26], and [27].

schematically in Figs. 1.7 and 1.8.

Chapter 3: Dephasing of entangled electron-hole pairs in a degenerate electron gas

We continue our investigation of the electron-hole entangler, to include the effects of dephasing. Dephasing appears because the electron and hole are coupled to other particles such as phonons and other electrons. Tracing out these other degrees of freedom corresponds to a transition from a pure electron-hole pair to a mixture. In this chapter, we investigate the loss of electron-hole entanglement due to this transition. Both the maximal violation $\mathcal{E}_{\max}$ of the Bell-CHSH inequality and the concurrence $\mathcal{C}$ are calculated. Entangled electron-hole states exist that can not violate the Bell-CHSH inequality.

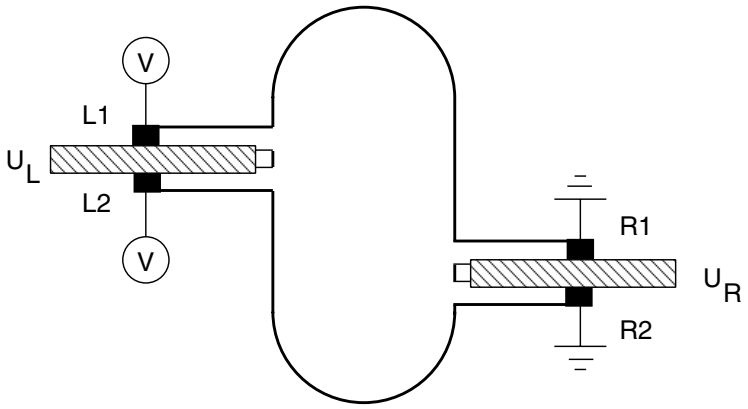

(a)

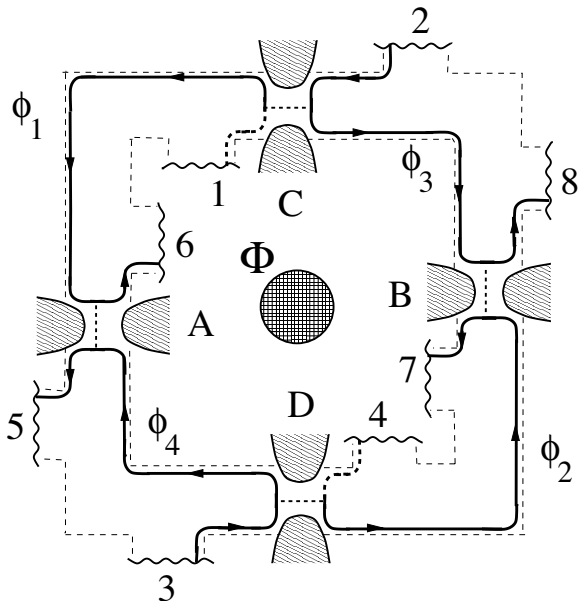

(b)

Figure 1.8: Two geometries to produce and detect orbital entanglement in zero magnetic field (a) and in the quantum Hall effect regime (b). Panels a and b are taken, respectively, from Refs. [28] and [29].

Chapter 4: Scattering theory of plasmon-assisted entanglement transfer and distillation

We now turn from electrons to photons. In chapter 4, the quantum mechanical limits to the plasmon-assisted entanglement transfer observed in [2] are analyzed. The experimental setup is indicated schematically in Fig. 1.9. It consists of a nonlinear crystal generating a pair of polarization-entangled photons. Subsequently, each photon passes through a metal plate perforated with arrays of holes smaller than the photon wavelength. On the metal plates, the entangled photons are each transformed into electron vibrations, called surface plasmons. The re-emitted photons are found to be still highly entangled. This signifies that after emission of a photon, the metal plate from which it originates does not carry information about its polarization. A scattering theory of entanglement transfer is constructed accordingly. This involves *coherent* scattering, turning a pure state into a pure state. (This is in contrast to the dephasing studied in chapter 3, which corresponds to *incoherent* or inelastic scattering, turning a pure state into a mixed state.) We find that the polarization-entanglement of a scattered photon pair can be described by two ratio's τ_1, τ_2 of polarization-dependent transmission probabilities. A fully entangled incident state is transferred without degradation for $\tau_1 = \tau_2$, but a relatively large mismatch of τ_1 and τ_2 can be tolerated with a small reduction of entanglement. We also predict that fully entangled Bell pairs can be distilled out of partially entangled radiation if τ_1 and τ_2 satisfy a pair of inequalities.

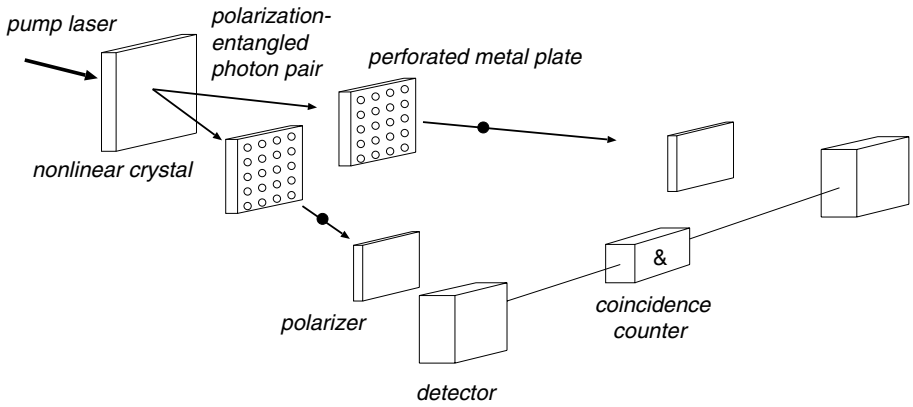

Figure 1.9: Schematic drawing of plasmon-assisted entanglement transfer, as in the experiment of Ref. [2].

Chapter 5: Transition from pure-state to mixed-state entanglement by random scattering

We continue our analysis of chapter 4 on the transfer of polarization-entanglement, to include the effect of multi-mode detection. Although the scattering is elastic and the scattered state pure, the observed two-photon polarization-state is generally mixed. This mixedness comes from the multi-mode detection, not from inelastic scattering like in chapter 3. Instead of the perforated metal plates of chapter 4, we consider scattering by disorder. Random matrix theory, applicable to disordered samples, allows us to find universal results — independent of microscopic details. Entanglement of the detected polarization-state is quantified by the concurrence $\mathcal{C}$ and maximal value of the Bell-CHSH parameter $\mathcal{E}_{\max}$. Both these quantities decay exponentially with the number of detected modes in case that the scattering mixes the polarization directions and algebraically if it does not.

Chapter 6: Entangling ability of a beam splitter in the presence of temporal which-path information

As mentioned in Sec. 1.2.2, the amount of polarization-entanglement induced by a beam splitter depends on the temporal indistinguishability of the photons. In this chapter, we establish the connection between temporal indistinguishability and the scattering matrix of the beam splitter in the formation of polarization-entanglement. We find that in the presence of photon-bunching, the interplay of the two kinds of "which-path" information — temporal and polarization — gives rise to the existence of entangled polarization-states that can not violate the Bell-CHSH inequality.

Bibliography

[1] M. A. Nielsen and I. L. Chuang, *Quantum Computation and Quantum Information* (Cambridge University Press, Cambridge, 2000).

[2] E. Altewischer, M. P. van Exter, and J. P. Woerdman, Nature **418**, 304 (2002).

[3] J. M. Elzerman, R. Hanson, L. H. Willems van Beveren, L. M. K. Vandersypen, and L. P. Kouwenhoven, in *Quantum Computation in Solid State Systems*, edited by P. Delsing, C. Granata, Y. Pashkin, B. Ruggiero, and P. Silvestrini (Springer, Berlin, 2006).

[4] A. Einstein, B. Podolsky, and N. Rosen, Phys. Rev. **47**, 777 (1935).

[5] J. S. Bell, Physics **1**, 195 (1964).

[6] J. F. Clauser, M. A. Horne, A. Shimony, and R. A. Holt, Phys. Rev. Lett. **23**, 880 (1969).

[7] C. H. Bennett, H. J. Bernstein, S. Popescu, and B. Schumacher, Phys. Rev. A **53**, 2046 (1996).

[8] N. Gisin, Phys. Lett. A **154**, 201 (1991).

[9] C. H. Bennett, D. P. DiVincenzo, J. A. Smolin, and W. K. Wootters, Phys. Rev. A **54**, 3824 (1996).

[10] W. K. Wootters, Phys. Rev. Lett. **80**, 2245 (1998).

[11] R. Horodecki, P. Horodecki, and M. Horodecki, Phys. Lett. A **200**, 340 (1995).

[12] F. Verstraete and M. M. Wolf, Phys. Rev. Lett. **89**, 170401 (2002).

[13] L. Mandel and E. Wolf, *Optical Coherence and Quantum Optics* (Cambridge University Press, Cambridge, 1995).

[14] M. S. Kim, W. Son, V. Bužek, and P. L. Knight, Phys. Rev. A **65**, 032323 (2002).

[15] W. Xiang-bin, Phys. Rev. A **66**, 024303 (2002).

[16] A. Aspect, P. Grangier, and G. Roger, Phys. Rev. Lett. **47**, 460 (1981).

[17] G. Burkard, D. Loss, and E. V. Sukhorukov, Phys. Rev. B **61**, 16303 (2000); D. Loss and E. V. Sukhorukov, Phys. Rev. Lett. **84**, 1035 (2000).

[18] W. D. Oliver, F. Yamaguchi, and Y. Yamamoto, Phys. Rev. Lett. **88**, 037901 (2002).

[19] D. S. Saraga and D. Loss, Phys. Rev. Lett. **90**, 166803 (2003).

[20] M. Blaauboer and D. P. DiVincenzo, cond-mat/0502060.

[21] G. B. Lesovik, T. Martin, and G. Blatter, Eur. Phys. J. B **24**, 287 (2001).

[22] P. Recher, E. V. Sukhorukov, and D. Loss, Phys. Rev. B **63**, 165314 (2001); P. Recher and D. Loss, Phys. Rev. B **65**, 165327 (2002).

[23] C. Bena, S. Vishveshwara, L. Balents, and M. P. A. Fisher, Phys. Rev. Lett. **89**, 037901 (2002).

[24] C. W. J. Beenakker, C. Emary, M. Kindermann, and J. L. van Velsen, Phys. Rev. Lett. **91**, 147901 (2003).

[25] A. V. Lebedev, G. B. Lesovik, and G. Blatter, Phys. Rev. B **71**, 045306 (2005).

[26] A. V. Lebedev, G. Blatter, C. W. J. Beenakker, and G. B. Lesovik, Phys. Rev. B **69**, 235312 (2004).

[27] A. Di Lorenzo and Yu. V. Nazarov, Phys. Rev. Lett. **94**, 210601 (2005).

[28] C. W. J. Beenakker, M. Kindermann, C. M. Marcus, and A. Yacoby, in *Fundamental Problems of Mesoscopic Physics*, edited by I. V. Lerner, B.L. Altshuler, and Y. Gefen, NATO Science Series II. Vol. 154 (Kluwer, Dordrecht, 2004).

[29] P. Samuelsson, E. V. Sukhorukov, and M. Büttiker, Phys. Rev. Lett. **92**, 026805 (2004).

Chapter 2

Production and detection of entangled electron-hole pairs in a degenerate electron gas

The controlled production and detection of entangled particles is the first step on the road towards quantum information processing [1]. In optics this step was taken long ago [2], but in the solid state it remains an experimental challenge. A variety of methods to entangle electrons have been proposed, based on quite different physical mechanisms [3]. A common starting point is a spin-singlet electron pair produced by interactions, such as the Coulomb interaction in a quantum dot [4–6], the pairing interaction in a superconductor [7–9], or Kondo scattering by a magnetic impurity [10]. A very recent proposal based on orbital entanglement also makes use of the superconducting pairing interaction [11].

It is known that photons can be entangled by means of linear optics using a beam splitter [12–14]. The electronic analogue would be an entangler that is based entirely on single-electron physics, without requiring interactions. But a direct analogy with optics fails: Electron reservoirs are in local thermal equilibrium, while in optics a beam splitter is incapable of entangling photons from a thermal source [15]. That is why previous proposals [10,16] to entangle electrons by means of a beam splitter start from a two-electron Fock state, rather than a many-electron thermal state. To control the extraction of a single pair of electrons from an electron reservoir requires strong Coulomb interaction in a tightly confined area, such as a semiconductor quantum dot or carbon nanotube [3]. Indeed, it has been argued [17] that one can not entangle a spatially separated current of electrons from a normal (not-superconducting) source without recourse to inter-

actions.

What we would like to propose here is an altogether different, interaction-free source of entangled quasiparticles in the solid state. The entanglement is not between electron pairs but between electron-hole pairs in a degenerate electron gas. The entanglement and spatial separation are realized purely by elastic scattering at a tunnel barrier in a two-channel conductor. We quantify the degree of entanglement by calculating how much the current fluctuations violate a Bell inequality.

Any two-channel conductor containing a tunnel barrier could be used in principle for our purpose, and the analysis which follows applies generally. The particular implementation described in Fig. 2.1 uses edge channel transport in the integer quantum Hall effect [18]. It has the advantage that the individual building blocks have already been realized experimentally for different purposes. If the two edge channels lie in the same Landau level, then the entanglement is between the spin degrees of freedom. Alternatively, if the spin degeneracy is not resolved by the Zeeman energy and the two edge channels lie in different Landau levels, then the entanglement is between the orbital degrees of freedom. The beam splitter is formed by a split gate electrode, as in Ref. [19]. In Fig. 2.1 we show the case that the beam splitter is weakly transmitting and strongly reflecting, but it could also be the other way around. To analyze the Bell inequality an extra pair of gates mixes the orbital degrees of freedom of the outgoing states independently of the incoming states. (Alternatively, one could apply a local inhomogeneity in the magnetic field to mix the spin degrees of freedom.) Finally, the current in each edge channel can be measured separately by using their spatial separation, as in Ref. [20]. (Alternatively, one could use the ferromagnetic method to measure spin current described in Ref. [3].)

Electrons are incident on the beam splitter from the left in a range eV above the Fermi energy E_F. (The states below E_F are all occupied at low temperatures, so they do not contribute to transport properties.) The incident state has the form

$$|\Psi_{\rm in}\rangle = \prod_{0<\varepsilon<eV} a^\dagger_{{\rm in},1}(\varepsilon) a^\dagger_{{\rm in},2}(\varepsilon)|0\rangle. \tag{2.1}$$

The fermion creation operator $a^\dagger_{{\rm in},i}(\varepsilon)$ excites the i-th channel incident from the left at energy ε above the Fermi level. Similarly, $b^\dagger_{{\rm in},i}(\varepsilon)$ excites a channel incident from the right. Each excitation is normalized such that it carries unit current. It is convenient to collect the creation operators in two vectors $a^\dagger_{\rm in}$, $b^\dagger_{\rm in}$ and to use a

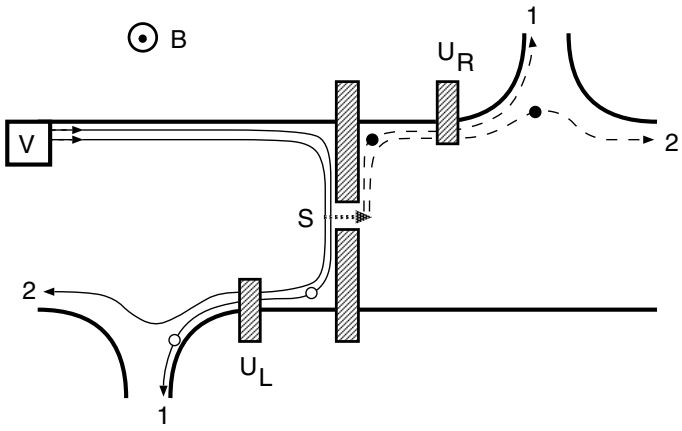

Figure 2.1: Schematic description of the method to produce and detect entangled edge channels in the quantum Hall effect. The thick black lines indicate the boundaries of a two-dimensional electron gas. A strong perpendicular magnetic field B ensures that the transport near the Fermi level E_F takes place in two edge channels, extended along a pair of equipotentials (thin solid and dashed lines, with arrows that give the direction of propagation). A split gate electrode (dashed rectangles at the center) divides the conductor into two halves, coupled by tunneling through a narrow opening (dashed arrow, scattering matrix S). If a voltage V is applied between the two halves, then there is a narrow energy range eV above E_F in which the edge channels are predominantly filled in the left half (solid lines) and predominantly empty in the right half (dashed lines). Tunneling events introduce filled states in the right half (black dots) and empty states in the left half (open circles). The entanglement of these particle-hole excitations is detected by the violation of a Bell inequality. This requires two gate electrodes to locally mix the edge channels (scattering matrices U_L, U_R) and two pair of contacts $1,2$ to separately measure the current in each transmitted and reflected edge channel.

matrix notation,

$$|\Psi_{\rm in}\rangle = \prod_{\varepsilon} \begin{pmatrix} a^\dagger_{\rm in} \\ b^\dagger_{\rm in} \end{pmatrix} \begin{pmatrix} \frac{1}{2}\sigma_y & 0 \\ 0 & 0 \end{pmatrix} \begin{pmatrix} a^\dagger_{\rm in} \\ b^\dagger_{\rm in} \end{pmatrix} |0\rangle, \tag{2.2}$$

with σ_y a Pauli matrix.

The input-output relation of the beam splitter is

$$\begin{pmatrix} a_{\rm out} \\ b_{\rm out} \end{pmatrix} = \begin{pmatrix} r & t' \\ t & r' \end{pmatrix} \begin{pmatrix} a_{\rm in} \\ b_{\rm in} \end{pmatrix}. \tag{2.3}$$

The 4×4 unitary scattering matrix S has 2×2 submatrices r, r', t, t' that describe reflection and transmission of states incident from the left or from the right. Substitution of Eq. (2.3) into Eq. (2.2) gives the outgoing state

$$|\Psi_{\rm out}\rangle = \prod_{\varepsilon} \big(a^\dagger_{\rm out} r\sigma_y t^{\rm T} b^\dagger_{\rm out} + [r\sigma_y r^{\rm T}]_{12} a^\dagger_{{\rm out},1} a^\dagger_{{\rm out},2} + [t\sigma_y t^{\rm T}]_{12} b^\dagger_{{\rm out},1} b^\dagger_{{\rm out},2} \big) |0\rangle. \tag{2.4}$$

The superscript "T" indicates the transpose of a matrix.

To identify the entangled electron-hole excitations we transform from particle to hole operators at the left of the beam splitter: $c_{{\rm out},i} = a^\dagger_{{\rm out},i}$. The new vacuum state is $a^\dagger_{{\rm out},1} a^\dagger_{{\rm out},2}|0\rangle$. To leading order in the transmission matrix the outgoing state becomes

$$|\Psi_{\rm out}\rangle = \prod_{\varepsilon} \big(\sqrt{w}|\Phi\rangle + \sqrt{1-w}|0\rangle \big), \tag{2.5}$$

$$|\Phi\rangle = w^{-1/2} c^\dagger_{\rm out} \gamma b^\dagger_{\rm out}|0\rangle, \;\; \gamma = \sigma_y r \sigma_y t^{\rm T}. \tag{2.6}$$

It represents a superposition of the vacuum state and a particle-hole state Φ with weight $w = {\rm Tr}\,\gamma\gamma^\dagger$.

The degree of entanglement of Φ is quantified by the concurrence [21, 22],

$$\mathcal{C} = 2\sqrt{{\rm Det}\,\gamma\gamma^\dagger}/{\rm Tr}\,\gamma\gamma^\dagger, \tag{2.7}$$

which ranges from 0 (no entanglement) to 1 (maximal entanglement). Substituting Eq. (2.6) and using the unitarity of the scattering matrix we find after some algebra that

$$\mathcal{C} = \frac{2\sqrt{(1-T_1)(1-T_2)T_1T_2}}{T_1+T_2-2T_1T_2} \approx 2\sqrt{T_1T_2}/(T_1+T_2) \;\text{ if }\; T_1, T_2 \ll 1. \tag{2.8}$$

The concurrence is entirely determined by the eigenvalues $T_1, T_2 \in (0,1)$ of the transmission matrix product $t^\dagger t = \mathbb{1} - r^\dagger r$. The eigenvectors do not contribute.

Maximal entanglement is achieved if the two transmission eigenvalues are equal: $\mathcal{C} = 1$ if $T_1 = T_2$.

The particle-hole entanglement is a nonlocal correlation that can be detected through the violation of a Bell inequality. We follow the formulation in terms of irreducible current correlators of Samuelsson, Sukhorukov, and Büttiker [11]. In the tunneling regime considered here that formulation is equivalent to the original formulation in terms of coincidence counting rates [23]. The tunneling assumption is essential: If T_1, T_2 are not $\ll 1$ one can not violate the Bell inequality without coincidence detection [17].

The quantity $C_{ij} = \int_{-\infty}^{\infty} dt\, \overline{\delta I_{L,i}(t) \delta I_{R,j}(0)}$ correlates the time-dependent current fluctuations $\delta I_{L,i}$ in channel $i = 1,2$ at the left with the current fluctuations $\delta I_{R,j}$ in channel $j = 1,2$ at the right. It can be measured directly in the frequency domain as the covariance of the low-frequency component of the current fluctuations. At low temperatures ($kT \ll eV$) the correlator has the general expression [24]

$$C_{ij} = -(e^3 V/h)|(rt^\dagger)_{ij}|^2. \tag{2.9}$$

We need the following rational function of correlators:

$$E = \frac{C_{11} + C_{22} - C_{12} - C_{21}}{C_{11} + C_{22} + C_{12} + C_{21}} = \frac{\mathrm{Tr}\, \sigma_z r t^\dagger \sigma_z t r^\dagger}{\mathrm{Tr}\, r^\dagger r t^\dagger t}. \tag{2.10}$$

By mixing the channels locally in the left and right arm of the beam splitter, the transmission and reflection matrices are transformed as $r \to U_L r$, $t \to U_R t$, with unitary 2×2 matrices U_L, U_R. The correlator transforms as

$$E(U_L, U_R) = \frac{\mathrm{Tr}\, U_L^\dagger \sigma_z U_L r t^\dagger U_R^\dagger \sigma_z U_R t r^\dagger}{\mathrm{Tr}\, r^\dagger r t^\dagger t}. \tag{2.11}$$

The Bell-CHSH (Clauser-Horne-Shimony-Holt) parameter is [23, 25]

$$\mathcal{E} = E(U_L, U_R) + E(U_L', U_R) + E(U_L, U_R') - E(U_L', U_R'). \tag{2.12}$$

The state is entangled if $|\mathcal{E}| > 2$ for some set of unitary matrices U_L, U_R, U_L', U_R'. By repeating the calculation of Ref. [26] we find the maximum [27]

$$\mathcal{E}_{\max} = 2[1 + 4T_1 T_2 (T_1 + T_2)^{-2}]^{1/2} > 2. \tag{2.13}$$

Comparison with Eq. (2.8) confirms the expected relation $\mathcal{E}_{\max} = 2(1 + \mathcal{C}^2)^{1/2}$ between the concurrence and the maximal violation of the CHSH inequality [28].

In conclusion, we have demonstrated theoretically that a tunnel barrier creates spatially separated currents of entangled electron-hole pairs in a degenerate

electron gas. Because no Coulomb or pairing interaction is involved, this is an attractive alternative to existing proposals for the interaction-mediated production of entanglement in the solid state. We have described a possible realization using edge channel transport in the quantum Hall effect, which makes use of existing technology. There is a remarkable contrast with quantum optics, where a beam splitter can not create entanglement if the source is in local thermal equilibrium. This might well explain why the elementary mechanism for entanglement production described here was not noticed before.

Bibliography

[1] B. M. Terhal, M. M. Wolf, and A. C. Doherty, Physics Today (April, 2003): p. 46.

[2] A. Aspect, P. Grangier, and G. Roger, Phys. Rev. Lett. **47**, 460 (1981).

[3] T. Martin, A. Crepieux, and N. Chtchelkatchev, in *Quantum Noise in Mesoscopic Physics*, edited by Yu. V. Nazarov, NATO Science Series II Vol. 97 (Kluwer, Dordrecht, 2003), p. 313; J. C. Egues, P. Recher, D. S. Saraga, V. N. Golovach, G. Burkard, E. V. Sukhorukov, and D. Loss, *ibid.*, p. 241.

[4] G. Burkard, D. Loss, and E. V. Sukhorukov, Phys. Rev. B **61**, R16303 (2000); D. Loss and E. V. Sukhorukov, Phys. Rev. Lett. **84**, 1035 (2000).

[5] W. D. Oliver, F. Yamaguchi, and Y. Yamamoto, Phys. Rev. Lett. **88**, 037901 (2002).

[6] D. S. Saraga and D. Loss, Phys. Rev. Lett. **90**, 166803 (2003).

[7] G. B. Lesovik, T. Martin, and G. Blatter, Eur. Phys. J. B **24**, 287 (2001).

[8] P. Recher, E. V. Sukhorukov, and D. Loss, Phys. Rev. B **63**, 165314 (2001); P. Recher and D. Loss, Phys. Rev. B **65**, 165327 (2002).

[9] C. Bena, S. Vishveshwara, L. Balents, and M. P. A. Fisher, Phys. Rev. Lett. **89**, 037901 (2002).

[10] A. T. Costa, Jr. and S. Bose, Phys. Rev. Lett. **87**, 277901 (2001).

[11] P. Samuelsson, E. V. Sukhorukov, and M. Büttiker, Phys. Rev. Lett. **91**, 157002 (2003).

[12] E. Knill, R. Laflamme, and G. J. Milburn, Nature **409**, 46 (2001).

[13] S. Scheel and D.-G. Welsch, Phys. Rev. A **64**, 063811 (2001).

[14] M. S. Kim, W. Son, V. Bužek, and P. L. Knight, Phys. Rev. A **65**, 032323 (2002).

[15] W. Xiang-bin, Phys. Rev. A **66**, 024303 (2002).

[16] S. Bose and D. Home, Phys. Rev. Lett. **88**, 050401 (2002).

[17] N. M. Chtchelkatchev, G. Blatter, G. B. Lesovik, and T. Martin, Phys. Rev. B **66**, 161320(R) (2002).

[18] C. W. J. Beenakker and H. van Houten, Solid State Phys. **44**, 1 (1991).

[19] M. Henny, S. Oberholzer, C. Strunk, T. Heinzel, K. Ensslin, M. Holland, and C. Schönenberger, Science **284**, 296 (1999).

[20] B. J. van Wees, E. M. M. Willems, C. J. P. M. Harmans, C. W. J. Beenakker, H. van Houten, J. G. Williamson, C. T. Foxon, and J. J. Harris, Phys. Rev. Lett. **62**, 1181 (1989).

[21] W. K. Wootters, Phys. Rev. Lett. **80**, 2245 (1998).

[22] The concurrence quantifies the entanglement per electron-hole pair. We have also calculated the entanglement of formation $\mathcal{F}$ (measured in bits per second) for the full state $\Psi_{\rm out}$ in Eq. (2.4). We find $\mathcal{F} = -(eV/h)[T_1 \log T_1(1-T_2) + T_2 \log T_2(1-T_1) + (1-T_1-T_2)\log(1-T_1)(1-T_2)]$. For $T_1, T_2 \ll 1$ this reduces to $\mathcal{F} \approx -(eV/h)[T_1 \log T_1 + T_2 \log T_2]$.

[23] J. S. Bell, Physics **1**, 195 (1964); J. F. Clauser, M. A. Horne, A. Shimony, and R. A. Holt, Phys. Rev. Lett. **23**, 880 (1969).

[24] M. Büttiker, Phys. Rev. Lett. **65**, 2901 (1990).

[25] Instead of searching for violations of the CHSH inequality $|\mathcal{E}| \leq 2$, one could equivalently consider the CH (Clauser-Horne) inequality $\mathcal{E}_{\rm CH} \leq 0$, with $\mathcal{E}_{\rm CH} = (-e^3V/h)^{-1}\{C_{ij}(U_L,U_R) + C_{ij}(U'_L,U_R) + C_{ij}(U_L,U'_R) - C_{ij}(U'_L,U'_R) - C_{i1}(U_L,\mathbb{1}) - C_{i2}(U_L,\mathbb{1}) - C_{1j}(\mathbb{1},U_R) - C_{2j}(\mathbb{1},U_R)\}$. Substituting $C_{ij}(U,V) = (-e^3V/h)|(Urt^\dagger V^\dagger)_{ij}|^2$ one obtains the relation $\mathcal{E}_{\rm CH} = \frac{1}{4}(\mathcal{E}-2){\rm Tr} rr^\dagger tt^\dagger$ between the CH and CHSH parameters.

[26] S. Popescu and D. Rohrlich, Phys. Lett. A **166**, 293 (1992).

[27] The maximum (2.13) is attained for $U_R = X$, $U'_R = 2^{-1/2}(\mathbb{1} + i\sigma_y)X$, $U_L = (\mathbb{1}\cos\alpha + i\sigma_y \sin\alpha)Y$, $U'_L = (\mathbb{1}\cos\alpha - i\sigma_y \sin\alpha)Y$, with $\tan 2\alpha = \mathcal{C}$. The unitary matrices X, Y are chosen such that $Yrt^{\dagger}X^{\dagger}$ is real diagonal.

[28] N. Gisin, Phys. Lett. A **154**, 201 (1991).

Chapter 3

Dephasing of entangled electron-hole pairs in a degenerate electron gas

3.1 Introduction

The production and detection of entangled particles is the essence of quantum information processing [1]. In optics, this is well-established with polarization-entangled photon pairs, but in the solid state it remains an experimental challenge. There exist several theoretical proposals for the production and detection of entangled electrons [2, 3]. These theoretical works address mainly pure states. The purpose of this chapter is to investigate what happens if the state is mixed. Some aspects of this problem were also considered in Refs. [4, 5]. We go a bit further by comparing violation of the Bell inequality to the degree of entanglement of the mixed state.

The entanglement scheme that we will analyze here, proposed in chapter 2, involves the Landau level index of an electron and hole quasiparticle (see Fig. 2.1). We consider one specific mechanism for the loss of purity, namely interaction with the environment. We model this interaction phenomenologically by introducing phase factors in the scattering matrix and subsequently averaging over these phases. A more microscopic treatment (for example along the lines of a recent paper [6]) is not attempted here. Another kind of mixture would result from energy averaging [7]. We assume that the applied voltage is sufficiently small that we can neglect energy averaging. Experimentally, both energy and phase averaging may play a role [8].

3.2 Dephasing

Dephasing is introduced phenomenologically through random phase shifts ϕ_i (ψ_i) accumulated in channel i at the left (right) of the tunnel barrier. The reflection and transmission matrices r and t transform as

$$r \to \begin{pmatrix} e^{i\phi_1} & 0 \\ 0 & e^{i\phi_2} \end{pmatrix} r_0, \;\; t \to \begin{pmatrix} e^{i\psi_1} & 0 \\ 0 & e^{i\psi_2} \end{pmatrix} t_0. \tag{3.1}$$

By averaging over the phase shifts, with distribution $P(\phi_1,\phi_2,\psi_1,\psi_2)$, and projecting out the vacuum contribution, the pure electron-hole excitation is converted into a mixture described by a 4×4 density matrix

$$\rho_{ij,kl} = \frac{\langle \gamma_{ij}\gamma^*_{kl}\rangle}{\langle \mathrm{Tr}\,\gamma\gamma^\dagger\rangle}. \tag{3.2}$$

Here $\langle\cdots\rangle$ denotes the average over the phases and the matrix γ refers to an electron-hole excitation cf. Eq. (2.6). The degree of entanglement is quantified by the concurrence $\mathcal{C}$, given by [9]

$$\mathcal{C} = \max\left\{0, \sqrt{\lambda_1} - \sqrt{\lambda_2} - \sqrt{\lambda_3} - \sqrt{\lambda_4}\right\}. \tag{3.3}$$

The λ_i's are the eigenvalues of the matrix product $\rho\cdot(\sigma_y\otimes\sigma_y)\cdot\rho^*\cdot(\sigma_y\otimes\sigma_y)$, in the order $\lambda_1\geq\lambda_2\geq\lambda_3\geq\lambda_4$. The concurrence ranges from 0 (no entanglement) to 1 (maximal entanglement).

The entanglement of the particle-hole excitations is detected by the violation of the Bell-CHSH (Clauser-Horne-Shimony-Holt) inequality [10, 11]. This requires two gate electrodes to locally mix the edge channels (scattering matrices U_L, U_R) and two pairs of contacts 1,2 to separately measure the current fluctuations $\delta I_{L,i}$ and $\delta I_{R,i}$ ($i=1,2$) in each transmitted and reflected edge channel. In the tunneling regime the Bell inequality can be formulated in terms of the low-frequency noise correlator [5]

$$C_{ij} = \int_{-\infty}^{\infty} dt\, \overline{\delta I_{L,i}(t)\delta I_{R,j}(0)}. \tag{3.4}$$

At low temperatures ($kT \ll eV$) the correlator has the general expression [12]

$$C_{ij}(U_L,U_R) = -(e^3V/h)\left|\left(U_L r t^\dagger U_R^\dagger\right)_{ij}\right|^2. \tag{3.5}$$

We again introduce the random phase shifts into r and t and average the correlator. The Bell-CHSH parameter is

$$\mathcal{E} = |E(U_L,U_R)+E(U'_L,U_R)+E(U_L,U'_R)-E(U'_L,U'_R)|, \tag{3.6}$$

where $E(U,V)$ is related to the average correlators $\langle C_{ij}(U,V)\rangle$ by

$$E = \frac{\langle C_{11}+C_{22}-C_{12}-C_{21}\rangle}{\langle C_{11}+C_{22}+C_{12}+C_{21}\rangle}. \tag{3.7}$$

The state is entangled if $\mathcal{E} > 2$ for some set of 2×2 unitary matrices U_L, U_R, U'_L, U'_R. If $\mathcal{E} = 2\sqrt{2}$ the entanglement is maximal.

3.3 Calculation of the mixed-state entanglement

We simplify the problem by assuming that the two transmission eigenvalues (eigenvalues of $tt^\dagger$) are identical: $T_1 = T_2 \equiv T$. In the absence of dephasing the electron and hole then form a maximally entangled pair. The transmission matrix $t_0 = T^{1/2}V$ and reflection matrix $r_0 = (1-T)^{1/2}V'$ in this case are equal to a scalar times a unitary matrix V, V'. Any 2×2 unitary matrix Ω can be parameterized by

$$\Omega = e^{i\theta}\begin{pmatrix} e^{i\alpha} & 0 \\ 0 & e^{-i\alpha}\end{pmatrix}\begin{pmatrix} \cos\xi & \sin\xi \\ -\sin\xi & \cos\xi\end{pmatrix}\begin{pmatrix} e^{i\beta} & 0 \\ 0 & e^{-i\beta}\end{pmatrix}, \tag{3.8}$$

in terms of four real parameters α,β,θ,ξ. The angle ξ governs the extent to which Ω mixes the degrees of freedom (no mixing for $\xi = 0,\pi/2$, complete mixing for $\xi = \pi/4$).

If we set $\Omega = \sigma_y V'\sigma_y V^{\mathrm{T}}$ we obtain for the matrix γ of Eq. (2.6) the parametrization

$$\gamma = e^{i\theta}\sqrt{T(1-T)}\begin{pmatrix} e^{i\phi_2+i\alpha} & 0 \\ 0 & e^{i\phi_1-i\alpha}\end{pmatrix}\begin{pmatrix} \cos\xi & \sin\xi \\ -\sin\xi & \cos\xi\end{pmatrix}\begin{pmatrix} e^{i\psi_1+i\beta} & 0 \\ 0 & e^{i\psi_2-i\beta}\end{pmatrix}. \tag{3.9}$$

In the same parametrization, the matrix $rt^\dagger$ which appears in Eq. (3.5) takes the form

$$rt^\dagger = e^{i\theta'-i\theta}\sqrt{T(1-T)}\times \begin{pmatrix} e^{i\phi_1-i\alpha} & 0 \\ 0 & e^{i\phi_2+i\alpha}\end{pmatrix}\begin{pmatrix} \cos\xi & \sin\xi \\ -\sin\xi & \cos\xi\end{pmatrix}\begin{pmatrix} e^{-i\psi_1-i\beta} & 0 \\ 0 & e^{-i\psi_2+i\beta}\end{pmatrix}, \tag{3.10}$$

with $e^{i\theta'} = \mathrm{Det}\, V'$. We have used the identity $V'V^\dagger = (\mathrm{Det}\, V')(\sigma_y V' \sigma_y V^{\mathrm{T}})^*$ to relate the parametrization of $rt^\dagger$ to that of γ. Note that

$$\mathrm{Tr}\,\gamma\gamma^\dagger = 2T(1-T) = \mathrm{Tr}\, rt^\dagger tr^\dagger, \tag{3.11}$$

independent of the phase shifts ϕ_i and ψ_i.

To average the phase factors we assume that the phase shifts at the left and the right of the tunnel barrier are independent, so

$$P(\phi_1,\phi_2,\psi_1,\psi_2) = P_L(\phi_1,\phi_2)P_R(\psi_1,\psi_2). \tag{3.12}$$

The complex dephasing parameters η_L and η_R are defined by

$$\eta_L = \int d\phi_1 \int d\phi_2\, P_L(\phi_1,\phi_2)e^{i\phi_1 - i\phi_2}, \quad \eta_R = \int d\psi_1 \int d\psi_2\, P_R(\psi_1,\psi_2)e^{i\psi_1 - i\psi_2}. \tag{3.13}$$

The density matrix (3.2) of the mixed particle-hole state has, in the parametrization (3.9), the elements

$$\rho = \frac{1}{2}\begin{pmatrix} \cos^2\xi & \tilde\eta_R\cos\xi\sin\xi & -\tilde\eta_L^*\cos\xi\sin\xi & \tilde\eta_L^*\tilde\eta_R\cos^2\xi \\ \tilde\eta_R^*\cos\xi\sin\xi & \sin^2\xi & -\tilde\eta_L^*\tilde\eta_R^*\sin^2\xi & \tilde\eta_L^*\cos\xi\sin\xi \\ -\tilde\eta_L\cos\xi\sin\xi & -\tilde\eta_L\tilde\eta_R\sin^2\xi & \sin^2\xi & -\tilde\eta_R\cos\xi\sin\xi \\ \tilde\eta_L\tilde\eta_R^*\cos^2\xi & \tilde\eta_L\cos\xi\sin\xi & -\tilde\eta_R^*\cos\xi\sin\xi & \cos^2\xi \end{pmatrix}. \tag{3.14}$$

We have defined $\tilde\eta_L = \eta_L e^{-2i\alpha}$, $\tilde\eta_R = \eta_R e^{2i\beta}$. The concurrence $\mathcal{C}$, calculated from Eq. (3.3), has a complicated expression. For $|\eta_L| = |\eta_R| \equiv \eta$ it simplifies to

$$\mathcal{C} = \max\left\{0, -\frac{1}{2}(1-\eta^2) + \frac{1}{4}\sqrt{16\eta^2 + 2(1-\eta^2)^2(1+\cos 4\xi)}\right\}. \tag{3.15}$$

Notice that $\mathcal{C} = \eta^2$ for $\xi = 0$.

For the Bell inequality we first note that the ratio of correlators (3.7) can be written as

$$E(U_L,U_R) = \frac{1}{2T(1-T)}\,\langle \mathrm{Tr}\, U_L^\dagger \sigma_z U_L r t^\dagger U_R^\dagger \sigma_z U_R t r^\dagger\rangle. \tag{3.16}$$

We parameterize

$$U_L^\dagger \sigma_z U_L = n_{L,x}\sigma_x + n_{L,y}\sigma_y + n_{L,z}\sigma_z \equiv \hat n_L \cdot \vec\sigma, \tag{3.17}$$

$$U_R^\dagger \sigma_z U_R = n_{R,x}\sigma_x + n_{R,y}\sigma_y + n_{R,z}\sigma_z \equiv \hat n_R \cdot \vec\sigma, \tag{3.18}$$

in terms of two unit vectors $\hat{n}_L, \hat{n}_R$ and a vector $\vec{\sigma}$ of Pauli matrices

$$\sigma_x = \begin{pmatrix} 0 & 1 \\ 1 & 0 \end{pmatrix} \equiv \sigma_1, \ \sigma_y = \begin{pmatrix} 0 & -i \\ i & 0 \end{pmatrix} \equiv \sigma_2, \ \sigma_z = \begin{pmatrix} 1 & 0 \\ 0 & -1 \end{pmatrix} \equiv \sigma_3. \quad (3.19)$$

Substituting the parametrization (3.10), Eq. (3.16) takes the form

$$E(U_L, U_R) = \frac{1}{2}\mathrm{Tr} \begin{pmatrix} n_{L,z} & \tilde{\eta}_L^* \nu_L^* \\ \tilde{\eta}_L \nu_L & -n_{L,z} \end{pmatrix} \begin{pmatrix} \cos\xi & \sin\xi \\ -\sin\xi & \cos\xi \end{pmatrix} \times \begin{pmatrix} n_{R,z} & \tilde{\eta}_R^* \nu_R^* \\ \tilde{\eta}_R \nu_R & -n_{R,z} \end{pmatrix} \begin{pmatrix} \cos\xi & -\sin\xi \\ \sin\xi & \cos\xi \end{pmatrix}, \quad (3.20)$$

where we have abbreviated $\nu_L = n_{L,x} + i n_{L,y}$, $\nu_R = n_{R,x} + i n_{R,y}$.

Comparing Eqs. (3.14) and (3.20), we see that

$$E(U_L, U_R) = \mathrm{Tr}\, \rho\, (\hat{n}_L \cdot \vec{\sigma})^{\mathrm{T}} \otimes (\hat{n}_R \cdot \vec{\sigma}). \quad (3.21)$$

(The transpose appears because of the transformation from electron to hole operators at the left of the barrier.) This is an explicit demonstration that the noise correlator (3.7) measures the density matrix (3.2) of the projected electron-hole state — without the vacuum contribution.

The maximal value $\mathcal{E}_{\max}$ of the Bell-CHSH parameter (3.6) for an arbitrary mixed state was analyzed in Refs. [13, 14]. For a pure state with concurrence $\mathcal{C}$ one has simply $\mathcal{E}_{\max} = 2\sqrt{1+\mathcal{C}^2}$ [15]. For a mixed state there is no one-to-one relation between $\mathcal{E}_{\max}$ and $\mathcal{C}$. Depending on the density matrix, $\mathcal{E}_{\max}$ can take on values between $2\mathcal{C}\sqrt{2}$ and $2\sqrt{1+\mathcal{C}^2}$. The general formula

$$\mathcal{E}_{\max} = 2\sqrt{u_1 + u_2} \quad (3.22)$$

for the dependence of $\mathcal{E}_{\max}$ on ρ involves the two largest eigenvalues u_1, u_2 of the real symmetric 3×3 matrix $R^{\mathrm{T}} R$ constructed from $R_{kl} = \mathrm{Tr}\, \rho\, \sigma_k \otimes \sigma_l$. For our density matrix (3.14) we find from Eq. (3.22) a simple expression if $|\eta_L| = |\eta_R| \equiv \eta$. It reads

$$\mathcal{E}_{\max} = \sqrt{2}\sqrt{(1+\eta^2)^2 + (1-\eta^2)^2 \cos 4\xi}. \quad (3.23)$$

3.4 Discussion

The result $\mathcal{E}_{\max} = 2(1+\eta^4)^{1/2}$ which follows from Eq. (3.23) for $\xi = 0$ was found in Ref. [5] in a somewhat different context. This corresponds to the case that the two edge channels are not mixed at the tunnel barrier. The Bell-CHSH inequality

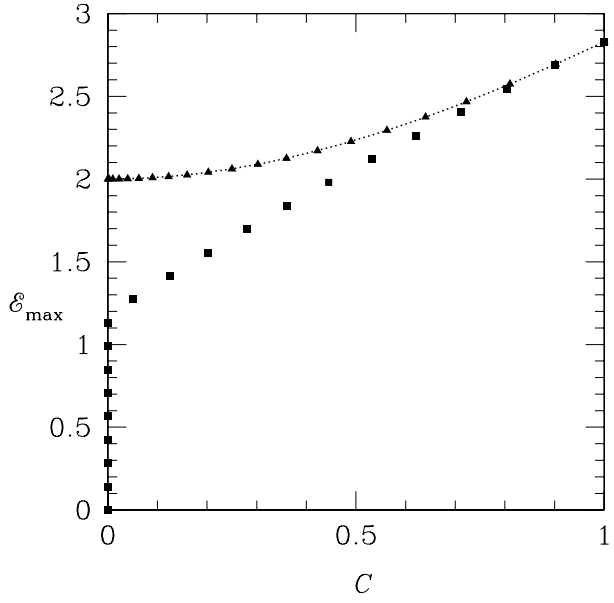

Figure 3.1: Relation between the maximal violation $\mathcal{E}_{\max}$ of the Bell-CHSH inequality and the concurrence $\mathcal{C}$ calculated from Eqs. (3.15) and (3.23) for mixing parameters $\xi = 0$ (triangles, no mixing) and $\xi = \frac{\pi}{4}$ (squares, complete mixing). The dephasing parameter η decreases from 1 (upper right corner, no dephasing) to 0 (lower left, complete dephasing) with steps of 0.05. The dotted line is the relation between $\mathcal{E}_{\max}$ and $\mathcal{C}$ for a pure state, which is also the largest possible value of $\mathcal{E}_{\max}$ for given $\mathcal{C}$.

$\mathcal{E}_{\max} \leq 2$ is then violated for arbitrarily strong dephasing. This is not true in the more general case $\xi \neq 0$, when $\mathcal{E}_{\max}$ drops below 2 at a finite value of η.

In Fig. 3.1 we compare $\mathcal{E}_{\max}$ and $\mathcal{C}$ for $\xi = 0$ (no mixing) and $\xi = \frac{\pi}{4}$ (complete mixing). For $\xi = 0$ the same relation $\mathcal{E}_{\max} = 2\sqrt{1+\mathcal{C}^2}$ between $\mathcal{E}_{\max}$ and $\mathcal{C}$ holds as for pure states (dotted curve). Violation of the Bell inequality is then equivalent to entanglement. For $\xi \neq 0$ there exist entangled states ($\mathcal{C} > 0$) without violation of the Bell inequality ($\mathcal{E}_{\max} \leq 2$). Violation of the Bell inequality is then a sufficient but not a necessary condition for entanglement. We define two characteristic dephasing parameters $\eta_{\mathcal{E}}$ and $\eta_{\mathcal{C}}$ by the smallest values such that

$$\mathcal{E}_{\max} > 2 \quad \text{for} \quad \eta > \eta_{\mathcal{E}}, \quad \mathcal{C} > 0 \quad \text{for} \quad \eta > \eta_{\mathcal{C}}. \tag{3.24}$$

The number $\eta_{\mathcal{E}}$ is the dephasing parameter below which Bell's inequality cannot be violated; The dephasing parameter $\eta_{\mathcal{C}}$ gives the border between entanglement and no entanglement. From Eqs. (3.15) and (3.23) we obtain

$$\eta_{\mathcal{C}} = \sqrt{\frac{5-\cos 4\xi - 2\sqrt{2}\sqrt{3-\cos 4\xi}}{1-\cos 4\xi}}, \quad \eta_{\mathcal{E}} = \sqrt{\frac{-1+\cos 4\xi + \sqrt{2-2\cos 4\xi}}{1+\cos 4\xi}}. \tag{3.25}$$

The two dephasing parameters are plotted in Fig. 3.2. The inequality $\eta_{\mathcal{E}} \geq \eta_{\mathcal{C}}$ reflects the fact that $\mathcal{E}_{\max}$ is an entanglement witness.

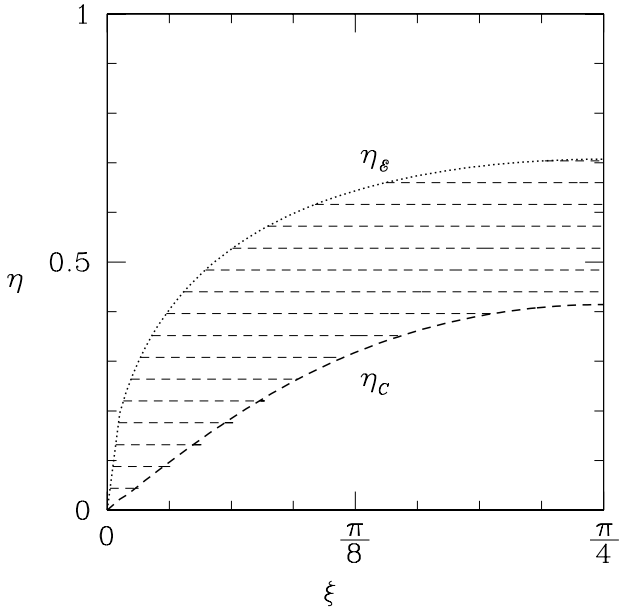

Figure 3.2: The Bell-CHSH inequality is violated for dephasing parameters $\eta > \eta_{\mathcal{E}}$, while entanglement is preserved for $\eta > \eta_{\mathcal{C}}$. The shaded region indicates dephasing and mixing parameters for which there is entanglement without violation of the Bell-CHSH inequality.

In conclusion, we have shown that the extent to which dephasing prevents the Bell inequality from detecting entanglement depends on the mixing of the degrees of freedom at the tunnel barrier. No mixing ($\xi = 0$) means that the maximally entangled electron-hole pair produced by the tunnel barrier is in one of the two

Bell states

$$|\psi_\alpha\rangle = \frac{1}{\sqrt{2}}(|\uparrow\downarrow\rangle + e^{i\alpha}|\downarrow\uparrow\rangle), \quad |\phi_\alpha\rangle = \frac{1}{\sqrt{2}}(|\uparrow\uparrow\rangle + e^{i\alpha}|\downarrow\downarrow\rangle). \tag{3.26}$$

(In our case the Landau level index $i = 1,2$ replaces the spin index $\uparrow$, $\downarrow$.) Then there is finite entanglement and finite violation of the Bell inequality for arbitrarily strong dephasing [5], and moreover there is the same one-to-one relation between degree of entanglement and violation of the Bell inequality as for pure states. All this no longer holds for non-zero mixing ($\xi \neq 0$), when the maximally entangled electron-hole pair is in a superposition of $|\phi_\alpha\rangle$ and $|\psi_{\alpha'}\rangle$. Then the entanglement disappears for a finite dephasing strength and the Bell inequality is no longer capable of unambiguously detecting entanglement.

Bibliography

[1] M. A. Nielsen and I. L. Chuang, *Quantum Computation and Quantum Information* (Cambridge University Press, Cambridge, 2000).

[2] J. C. Egues, P. Recher, D. S. Saraga, V. N. Golovach, G. Burkard, E. V. Sukhorukov, and D. Loss, in *Quantum Noise in Mesoscopic Physics*, edited by Yu. V. Nazarov, NATO Science Series II Vol. 97 (Kluwer, Dordrecht, 2003).

[3] T. Martin, A. Crepieux, and N. Chtchelkatchev, in *Quantum Noise in Mesoscopic Physics*, edited by Yu. V. Nazarov, NATO Science Series II Vol. 97 (Kluwer, Dordrecht, 2003).

[4] G. Burkard and D. Loss, Phys. Rev. Lett. **91**, 087903 (2003).

[5] P. Samuelsson, E. V. Sukhorukov, and M. Büttiker, Phys. Rev. Lett. **91**, 157002 (2003).

[6] F. Marquardt and C. Bruder, Phys. Rev. Lett. **92**, 056805 (2004).

[7] Referring to Fig. 2.1, consider the area A between the two equipotentials starting at U_L, through S, and ending at U_R. This enclosed area varies by δA when the energy of the equipotentials varies by eV. Dephasing results if $B\delta A \gtrsim h/e$. The ratio $\delta A/A \simeq V|\nabla\vec{E}|/|\vec{E}|^2$ depends on the gradient of the electric field $\vec{E}$ near the edge. For $B = 5\,\mathrm{T}$, $A = 10^{-13}\,\mathrm{m}^2$, one would need $V \lesssim 10^{-2}|\vec{E}|^2/|\nabla\vec{E}|$ to avoid dephasing by energy averaging.

[8] Y. Ji, Y. Chung, D. Sprinzak, M. Heiblum, D. Mahalu, and H. Shtrikman, Nature **422**, 415 (2003).

[9] W. K. Wootters, Phys. Rev. Lett. **80**, 2245 (1998).

[10] J. F. Clauser, M. A. Horne, A. Shimony, and R. A. Holt, Phys. Rev. Lett. **23**, 880 (1969).

[11] N. M. Chtchelkatchev, G. Blatter, G. B. Lesovik, and T. Martin, Phys. Rev. B **66**, 161320(R) (2002).

[12] M. Büttiker, Phys. Rev. Lett. **65**, 2901 (1990).

[13] R. Horodecki, P. Horodecki, and M. Horodecki, Phys. Lett. A **200**, 340 (1995).

[14] F. Verstraete and M. M. Wolf, Phys. Rev. Lett. **89**, 170401 (2002).

[15] N. Gisin, Phys. Lett. A **154**, 201 (1991).

Chapter 4

Scattering theory of plasmon-assisted entanglement transfer and distillation

The motivation for the work presented in this chapter came from the remarkable demonstration by Altewischer, Van Exter, and Woerdman of the transfer of quantum mechanical entanglement from photons to surface plasmons and back to photons [1]. Since entanglement is a highly fragile property of a two-photon state, it came as a surprise that this property could survive with little degradation the conversion to and from the macroscopic degrees of freedom in a metal [2].

We present a quantitative description of the finding of Ref. [1] that the entanglement is lost if it is measured during transfer, that is to say, if the medium through which the pair of polarization-entangled photons is passed acts as a "which-way" detector for polarization. Our analysis explains why a few percent degradation of entanglement could be realized without requiring a highly symmetric medium. We predict that the experimental setup of Ref. [1] could be used to "distill" [3, 4] fully entangled Bell pairs out of partially entangled incident radiation, and we identify the region in parameter space where this distillation is possible.

We assume that the medium is *linear*, so that its effect on the radiation can be described by a scattering matrix. The assumption of linearity of the interaction of radiation with surface plasmons is central to the literature on this topic [5–9]. We will not make any specific assumptions on the mode and frequency dependence of the scattering matrix, but extract the smallest number of independently measurable parameters needed to describe the experiment. By concentrating on

model-independent results we can isolate the fundamental quantum mechanical limitations on the entanglement transfer, from the limitations specific for any particular transfer mechanism.

The system considered is shown schematically in Fig. 4.1. Polarization-entangled radiation is scattered by two objects and detected by a pair of detectors behind the objects in the far-field. The objects used in Ref. [1] are metal films perforated by a square array of subwavelength holes. The transmission amplitude $t_{\sigma\sigma',i}$ of object $i = 1,2$ relates the transmitted radiation (with polarization $\sigma = \mathrm{H},\mathrm{V}$) to the incident radiation (polarization $\sigma' = \mathrm{H},\mathrm{V}$). We assume a single-mode incident beam and a single-mode detector (smaller than the coherence area), so that we require a set of eight transmission amplitudes $t_{\sigma\sigma',i}$ out of the entire scattering matrix (which also contains reflection amplitudes and transmission amplitudes to other modes). We do not require that the scattering matrix is unitary, so our results remain valid if the objects absorb part of the incident radiation. What is neglected is the thermal radiation, either from the two objects or from the electromagnetic environment of the detectors. This thermal noise is insignificant at room temperature and optical frequencies.

The radiation incident on the two objects is in a known, partially entangled state and we wish to determine the degree of entanglement of the detected radiation. It is convenient to use a matrix notation. The incident two-photon state has the general form

$$|\Psi_{\mathrm{in}}\rangle = a^{\mathrm{in}}_{\mathrm{HH}}|\mathrm{HH}\rangle + a^{\mathrm{in}}_{\mathrm{HV}}|\mathrm{HV}\rangle + a^{\mathrm{in}}_{\mathrm{VH}}|\mathrm{VH}\rangle + a^{\mathrm{in}}_{\mathrm{VV}}|\mathrm{VV}\rangle. \tag{4.1}$$

The four complex numbers $a^{\mathrm{in}}_{\sigma\sigma'}$ form a matrix

$$A_{\mathrm{in}} = \begin{pmatrix} a^{\mathrm{in}}_{\mathrm{HH}} & a^{\mathrm{in}}_{\mathrm{HV}} \\ a^{\mathrm{in}}_{\mathrm{VH}} & a^{\mathrm{in}}_{\mathrm{VV}} \end{pmatrix}. \tag{4.2}$$

Normalization of $|\Psi_{\mathrm{in}}\rangle$ requires $\mathrm{Tr}\, A_{\mathrm{in}} A^{\dagger}_{\mathrm{in}} = 1$.

The four transmission amplitudes $t_{\sigma\sigma',i}$ of object $i = 1,2$ form the matrix

$$T_i = \begin{pmatrix} t_{\mathrm{HH},i} & t_{\mathrm{HV},i} \\ t_{\mathrm{VH},i} & t_{\mathrm{VV},i} \end{pmatrix}. \tag{4.3}$$

The transmitted two-photon state $|\Psi_{\mathrm{out}}\rangle$ has matrix of coefficients

$$A_{\mathrm{out}} = Z^{-1/2} T_1 A_{\mathrm{in}} T_2^{\mathrm{T}}, \tag{4.4}$$

with normalization factor

$$Z = \mathrm{Tr}(T_1 A_{\mathrm{in}} T_2^{\mathrm{T}})(T_1 A_{\mathrm{in}} T_2^{\mathrm{T}})^{\dagger}. \tag{4.5}$$

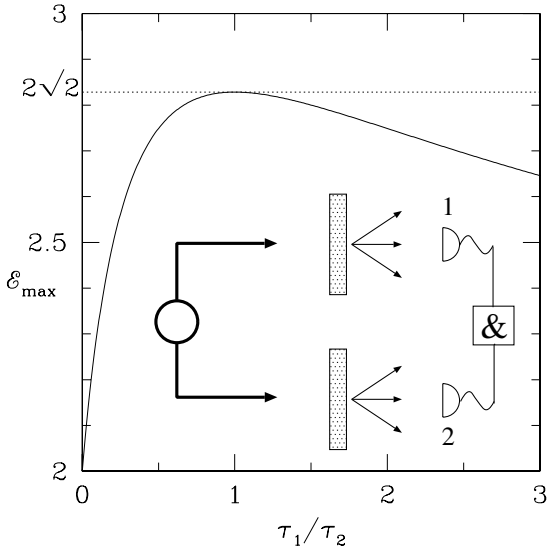

Figure 4.1: Main plot: Efficiency of the entanglement transfer for a fully entangled incident state, as given by Eq. (4.13). The maximal violation $\mathcal{E}_{\max}$ of Bell's inequality at the photodetectors is plotted as a function of the ratio $\tau_1/\tau_2 = T_{1+}T_{2-}/T_{1-}T_{2+}$ of the polarization-dependent transmission probabilities. The inset shows schematically the geometry of the experiment [1]. A pair of polarization-entangled photons is incident from the left on two perforated metal films. The photodetectors at the right, connected by a coincidence counter, measure the degree of entanglement of the transmitted radiation.

For a pure state $|\Psi\rangle$ the maximal value of the Bell-CHSH parameter $\mathcal{E}_{\max}$ [10] is related to the concurrence $\mathcal{C}$ [11] by $\mathcal{E}_{\max} = 2\sqrt{1+\mathcal{C}^2}$ [12]. In terms of a matrix A, the concurrence takes the form $\mathcal{C} = 2\,|\mathrm{Det}\,A|$ and ranges from 0 (no entanglement) to 1 (maximal entanglement). A fully entangled state could be the Bell pair $\big(|\mathrm{HV}\rangle - |\mathrm{VH}\rangle\big)/\sqrt{2}$, or any state derived from it by a local unitary transformation ($A \to UAV$ with U, V arbitrary unitary matrices). The degree of entanglement $\mathcal{C}_{\mathrm{in}} = 2|\mathrm{Det}\,A_{\mathrm{in}}|$ of the incident state is given and we seek the degree of entanglement $\mathcal{C}_{\mathrm{out}} = 2|\mathrm{Det}\,A_{\mathrm{out}}|$ of the transmitted state. We are particularly interested in the largest $\mathcal{C}_{\mathrm{out}}$ that can be reached by applying local unitary transformations to the incident state. This would correspond to the experimental situation that the

polarizations of the two incoming photons are rotated independently, in order to maximize the violation of Bell's inequality of the detected photon pair.

Before proceeding with the calculation we introduce some parametrizations. The Hermitian matrix product $T_i T_i^\dagger$ has the eigenvalue–eigenvector decomposition

$$T_1 T_1^\dagger = U^\dagger \begin{pmatrix} T_{1+} & 0 \\ 0 & T_{1-} \end{pmatrix} U, \;\; T_2 T_2^\dagger = V^\dagger \begin{pmatrix} T_{2+} & 0 \\ 0 & T_{2-} \end{pmatrix} V. \tag{4.6}$$

The matrices of eigenvectors U, V are unitary and the transmission eigenvalues $T_{i\pm}$ are real numbers between 0 and 1. We order them such that $0 \le T_{i-} \le T_{i+} \le 1$ for each $i = 1,2$. We will see that the maximal entanglement transfer depends only on the ratios $\tau_i = T_{i+}/T_{i-}$. This parametrization therefore extracts the two significant real numbers τ_1, τ_2 out of eight complex transmission amplitudes. The Hermitian matrix product $A_{\rm in} A_{\rm in}^\dagger$ has eigenvalues $\lambda_\pm = \frac{1}{2} \pm \frac{1}{2}(1 - \mathcal{C}_{\rm in}^2)^{1/2}$. These appear in the polar decomposition

$$U A_{\rm in} V = e^{i\phi} \begin{pmatrix} u_+ & u_- \\ -u_-^* & u_+^* \end{pmatrix} \begin{pmatrix} \sqrt{\lambda_+} & 0 \\ 0 & \sqrt{\lambda_-} \end{pmatrix} \begin{pmatrix} v_+ & v_- \\ -v_-^* & v_+^* \end{pmatrix}. \tag{4.7}$$

The phase ϕ is real and $u_\pm, v_\pm$ are complex numbers constrained by $|u_\pm| = (\frac{1}{2} \pm u)^{1/2}$, $|v_\pm| = (\frac{1}{2} \pm v)^{1/2}$, with real $u, v \in (-\frac{1}{2}, \frac{1}{2})$. These numbers can be varied by local unitary transformations, so later on we will want to choose values which maximize the detected entanglement.

With these parametrizations a calculation of the determinant of $A_{\rm out}$ leads to the following relation between $\mathcal{C}_{\rm in}$ and $\mathcal{C}_{\rm out}$:

$$\begin{aligned} \mathcal{C}_{\rm out} &= \frac{\mathcal{C}_{\rm in}\sqrt{\tau_1\tau_2}}{(\tau_1-1)(\tau_2-1)} \big[\lambda_+ Q_+ + \lambda_- Q_- \\ &- 2\sqrt{\lambda_+\lambda_-}(\tfrac{1}{4} - u^2)^{1/2}(\tfrac{1}{4} - v^2)^{1/2} \cos\Phi \big]^{-1}, \qquad (4.8) \\ Q_\pm &= \left(u \pm \tfrac{1}{2}\frac{\tau_1+1}{\tau_1-1} \right) \left(v \pm \tfrac{1}{2}\frac{\tau_2+1}{\tau_2-1} \right). \qquad (4.9) \end{aligned}$$

The phase Φ equals the argument of $u_+ u_-^* v_+ v_-$. To maximize $\mathcal{C}_{\rm out}$ we should choose $\Phi = 0$.

We first analyze this expression for the case of a fully entangled incident state, as in the experiment [1]. For $\mathcal{C}_{\rm in} = 1$ one has $\lambda_+ = \lambda_- = 1/2$, and Eq. (4.8) simplifies to

$$\begin{aligned} \mathcal{C}_{\rm out} &= \frac{4\sqrt{\tau_1\tau_2}}{(\tau_1+1)(\tau_2+1) + 4a(\tau_1-1)(\tau_2-1)}, \qquad (4.10) \\ a &= uv - (\tfrac{1}{4} - u^2)^{1/2}(\tfrac{1}{4} - v^2)^{1/2} \cos\Phi. \qquad (4.11) \end{aligned}$$

Since $\tau_i \geq 1$ and $|a| \leq \frac{1}{4}$ we conclude that the degree of entanglement is bounded by $\mathcal{C}_{\min} \leq \mathcal{C}_{\text{out}} \leq \mathcal{C}_{\max}$, with

$$\mathcal{C}_{\min} = \frac{2\sqrt{\tau_1\tau_2}}{1+\tau_1\tau_2}, \;\; \mathcal{C}_{\max} = \frac{2\sqrt{\tau_1/\tau_2}}{1+\tau_1/\tau_2}. \tag{4.12}$$

The maximum $\mathcal{C}_{\max}$ can always be reached by a proper choice of the (fully entangled) incident state, so the maximal violation of Bell's inequality is given by

$$\mathcal{E}_{\max} = 2\sqrt{1+\frac{4\tau_1/\tau_2}{(1+\tau_1/\tau_2)^2}}. \tag{4.13}$$

The dependence of $\mathcal{E}_{\max}$ on τ_1/τ_2 is plotted in Fig. 4.1. Full entanglement is obtained for $\tau_1 = \tau_2$, hence for $T_{1+}T_{2-} = T_{1-}T_{2+}$. Generically, this requires either identical objects ($T_{1\pm} = T_{2\pm}$) or non-identical objects with $T_{i+} = T_{i-}$. If $\tau_1 = \tau_2$ there are no "which-way" labels and entanglement fully survives with no degradation.

Small deviations of τ_1/τ_2 from unity only reduce the entanglement to second order,

$$\mathcal{E}_{\max} = 2\sqrt{2}\big[1 - \frac{1}{16}(\tau_1/\tau_2 - 1)^2 + \mathcal{O}(\tau_1/\tau_2 - 1)^3\big]. \tag{4.14}$$

So for a small reduction of the entanglement one can tolerate a large mismatch of the transmission probabilities. In particular, the experimental result $\mathcal{E} = 2.71$ for plasmon-assisted entanglement transfer [1] can be reached with more than a factor two of mismatch ($\mathcal{E} = 2.71$ for $\tau_1/\tau_2 = 2.4$).

As a simple example we calculate the symmetry parameter τ_1/τ_2 for a Lorentzian transmission probability, appropriate for plasmon-assisted entanglement transfer [5–9]. We take

$$T_{i\pm} = \frac{\mathcal{T}\,\Gamma^2}{(\omega_0 - \omega_{i\pm})^2 + \Gamma^2}, \tag{4.15}$$

where ω_0 is the frequency of the incident radiation, Γ is the linewidth, and $\mathcal{T}$ is the transmission probability at the resonance frequency $\omega_{i\pm}$. (For simplicity we take polarization-independent Γ and $\mathcal{T}$.) The transmission is through an optically thick metal film with a rectangular array of subwavelength holes (lattice constants $L_{i\pm}$). The dispersion relation of the surface plasmons is $\omega_{i\pm} = (1+1/\epsilon)^{1/2} 2\pi n c/L_{i\pm}$ [9], where ϵ is the real part of the dielectric constant and n is the order of the resonance, equal to the number of plasmon-field oscillations in a lattice constant. We break the symmetry by taking one square array of holes and one rectangular

array (lattice constants $L_0 = L_{1+} = L_{2+} = L_{2-}$ and $L_1 = L_{1-}$). The lattice constant L_0 is chosen such that the incident radiation is at resonance. The symmetry parameter becomes

$$\frac{\tau_1}{\tau_2} = 1 + (2\pi)^2 \left(\frac{nl}{L_0} - \frac{nl}{L_1} \right)^2, \quad l = \frac{c}{\Gamma} \sqrt{\frac{\epsilon + 1}{\epsilon}}. \tag{4.16}$$

The length l is the propagation length of the surface plasmon. (We have taken $c(1 + 1/\epsilon)^{1/2}$ for the plasmon group velocity, valid if ω_0 is not close to the plasma frequency [9].) Combining Eqs. (4.14) and (4.16) we see that the deviation of $\mathcal{E}_{\max}$ from $2\sqrt{2}$ (the degradation of the entanglement) is proportional to the *fourth* power of the difference between the number of oscillations of the plasmon field along the two lattice vectors.

Turning now to the more general case of a partially entangled incident state, we ask the following question: Is it possible to achieve $\mathcal{C}_{\text{out}} = 1$ even if $\mathcal{C}_{\text{in}} < 1$? In other words, can one detect a $2\sqrt{2}$ violation of Bell's inequality after transmission even if the original state was only partially entangled? Examination of Eq. (4.8) shows that the answer to this question is: *Yes*, provided τ_1 and τ_2 satisfy

$$\left| \ln \frac{\tau_1}{\tau_2} \right| \leq 2 \operatorname{arcosh}(\mathcal{C}_{\text{in}}^{-1}) \text{ and } \ln \tau_1 \tau_2 \geq 2 \operatorname{arcosh}(\mathcal{C}_{\text{in}}^{-1}). \tag{4.17}$$

The allowed values of τ_1 and τ_2 lie in a strip that is open at one end, see Fig. 4.2. The boundaries are reached at $|u| = |v| = \frac{1}{2}$. The region inside the strip is reached by choosing both $|u|$ and $|v| < 1/2$. For $\mathcal{C}_{\text{in}} = 1$ the strip collapses to the single line $\tau_1 = \tau_2$, in agreement with Eq. (4.12).

The possibility to achieve $\mathcal{C}_{\text{out}} = 1$ for $\mathcal{C}_{\text{in}} < 1$ is an example of distillation of entanglement [3, 4]. (See Refs. [13–16] for other schemes proposed recently, and Ref. [17] for an experimental realization.) As it should, no entanglement is created in this operation. Out of N incoming photon-pairs with entanglement $\mathcal{C}_{\text{in}}$ one detects NZ pairs with entanglement $\mathcal{C}_{\text{out}} = \mathcal{C}_{\text{in}} Z^{-1} \sqrt{T_{1+} T_{1-} T_{2+} T_{2-}}$, so that $NZ\mathcal{C}_{\text{out}} \leq N\mathcal{C}_{\text{in}}$.

In conclusion, we have shown that optical entanglement transfer and distillation through a pair of linear media can be described by two ratios τ_1 and τ_2 of polarization-dependent transmission probabilities. For fully entangled incident radiation, the maximal violation of Bell's inequality at the detectors is given by a function (4.13) of τ_1/τ_2 which decays only slowly around the optimal value $\tau_1/\tau_2 = 1$. Distillation of a fully entangled Bell pair out of partially entangled incident radiation is possible no matter how low the initial entanglement, provided that τ_1 and τ_2 satisfy the two inequalities (4.17).

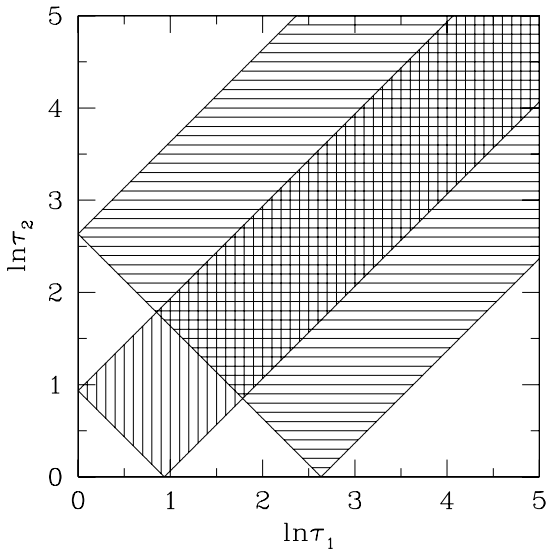

Figure 4.2: The shaded strips indicate the values of $\ln\tau_1$ and $\ln\tau_2$ for which $\mathcal{C}_{\rm out} = 1$ can be reached with $\mathcal{C}_{\rm in} = 0.5$ (horizontally shaded) and $\mathcal{C}_{\rm in} = 0.9$ (vertically shaded), in accordance with Eq. (4.17).

Our results provide a simple way to describe the experiment [1] on plasmon-assisted entanglement transfer, in terms of two separately measurable parameters. By changing the square array of holes used in Ref. [1] into a rectangular array (or, equivalently, by tilting the square array relative to the incident beam), one can move away from the point $\tau_1 = \tau_2 = 1$ and search for the entanglement distillation predicted here. The possibility to extract Bell pairs by manipulating surface plasmons may have interesting applications in quantum information processing.

Bibliography

[1] E. Altewischer, M. P. van Exter, and J. P. Woerdman, Nature **418**, 304 (2002).

[2] W. Barnes, Nature **418**, 281 (2002).

[3] C. H. Bennett, H. J. Bernstein, S. Popescu, and B. Schumacher, Phys. Rev. A **53**, 2046 (1996).

[4] M. A. Nielsen and I. L. Chuang, *Quantum Computation and Quantum Information* (Cambridge University Press, 2000).

[5] U. Schröter and D. Heitmann, Phys. Rev. B **58**, 15419 (1998).

[6] M. M. J. Treacy, Appl. Phys. Lett. **75**, 606 (1999).

[7] J. A. Porto, F. J. García-Vidal, and J. B. Pendry, Phys. Rev. Lett. **83**, 2845 (1999).

[8] L. Martín-Moreno, F. J. García-Vidal, H. J. Lezec, K. M. Pellerin, T. Thio, J. B. Pendry, and T. W. Ebbesen, Phys. Rev. Lett. **86**, 1114 (2001).

[9] H. Raether, *Surface Plasmons* (Springer, Berlin, 1988).

[10] J. F. Clauser, M. A. Horne, A. Shimony, and R. A. Holt, Phys. Rev. Lett. **23**, 880 (1969).

[11] W. K. Wootters, Phys. Rev. Lett. **80**, 2245 (1998).

[12] N. Gisin, Phys. Lett. A **154**, 201 (1991).

[13] H.-W. Lee and J. Kim, Phys. Rev. A **63**, 012305 (2000).

[14] D. Gottesman and J. Preskill, Phys. Rev. A **63**, 022309 (2001).

[15] T. Yamamoto, M. Koashi, and N. Imoto, Phys. Rev. A **64**, 012304 (2001).

[16] J.-W. Pan, C. Simon, C. Brukner, and A. Zeilinger, Nature **410**, 1067 (2001).

[17] P. G. Kwiat, S. Barraza-Lopez, A. Stefanov, and N. Gisin, Nature **409**, 1014 (2001).

Chapter 5

Transition from pure-state to mixed-state entanglement by random scattering

5.1 Introduction

A pair of photons in the Bell state $(|\mathrm{HV}\rangle + |\mathrm{VH}\rangle)/\sqrt{2}$ can be transported over long distances with little degradation of the entanglement of their horizontal (H) and vertical (V) polarizations. Polarization-dependent scattering has little effect on the degree of entanglement, as long as it remains linear (hence describable by a scattering matrix) and as long as the photons are detected in a single spatial mode only (chapter 4).

Polarization-dependent scattering may significantly degrade the entanglement in the case of multi-mode detection. Upon summation over N spatial modes the initially pure state of the Bell pair is reduced to a mixed state with respect to the polarization degrees of freedom. This loss of purity diminishes the entanglement — even if the two polarization directions are not mixed by the scattering.

The transition from pure-state to mixed-state entanglement will in general depend on the detailed form of the scattering matrix. However, a universal regime is entered in the case of randomly located scattering centra. This is the regime of applicability of random-matrix theory [1, 2]. As we will show in this chapter, the transmission of polarization-entangled radiation through disordered media reduces the degree of entanglement in a way which, on average, depends only on the number N of detected modes. (The average refers to an ensemble of disordered media with different random positions of the scatterers.) The degree of entan-

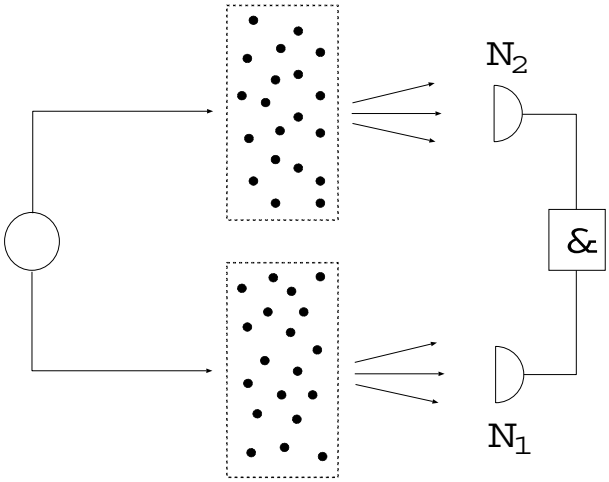

Figure 5.1: Schematic diagram of the transfer of polarization-entangled radiation through two disordered media. The degree of entanglement of the transmitted radiation is measured by two multi-mode photodetectors (N_i modes) in a coincidence circuit (represented by the box with & inside). The combination of polarization-dependent scattering and multi-mode detection causes a transition from a pure state to a mixed state in the polarization degrees of freedom, and a resulting decrease of the detected entanglement.

glement (as quantified either by the concurrence [3] or by the violation of a Bell inequality [4, 5]) decreases exponentially with N if the disorder randomly mixes the polarization directions. If the polarization is conserved, then the decrease is a power law ($\propto N^{-1}$ if both photons are scattered and $\propto N^{-1/2}$ if only one photon is scattered).

5.2 Formulation of the problem

We consider two beams of polarization-entangled photons (Bell pairs) that are scattered by two separate disordered media (see Fig. 5.1). Two photodetectors in a coincidence circuit measure the degree of entanglement of the transmitted radiation through the violation of a Bell inequality. The scattered Bell pair is in the pure state

$$\Psi_{n\sigma,m\tau} = \frac{1}{\sqrt{2}}\left(u^{+}_{n\sigma} v^{-}_{m\tau} + u^{-}_{n\sigma} v^{+}_{m\tau}\right). \tag{5.1}$$

The indices $n \in \{1,2,\dots M_1\}$, $m \in \{1,2,\dots M_2\}$ label the transverse spatial modes and the indices $\sigma,\tau \in \{+,-\}$ label the horizontal and vertical polarizations. The first pair of indices n,σ refers to the first photon and the second pair of indices m,τ refers to the second photon. The scattering amplitudes $u^{\pm}_{n\sigma}$ relate the incoming mode $(1,\pm)$ of the first photon to the outgoing mode (n,σ), and similarly for the second photon. The two vectors $(u^+_{1+},u^+_{2+},\dots u^+_{M_1+},u^+_{1-},u^+_{2-},\dots u^+_{M_1-})$ and $(u^-_{1+},u^-_{2+},\dots u^-_{M_1+},u^-_{1-},u^-_{2-},\dots u^-_{M_1-})$ of scattering amplitudes of the first photon are orthonormal, and similarly for the second photon.

A subset of N_1 out of the M_1 modes are detected in the first detector. We relabel the modes so that $n = 1,2,\dots N_1$ are the detected modes. This subset is contained in the four vectors $u^{++}_n \equiv u^+_{n+}$, $u^{+-}_n \equiv u^+_{n-}$, $u^{-+}_n \equiv u^-_{n+}$, $u^{--}_n \equiv u^-_{n-}$ of length N_1 each. We write these vectors in bold face, $\mathbf{u}_{\pm\pm}$, omitting the mode index. Similarly, the second detector detects N_2 modes, contained in vectors $\mathbf{v}_{\pm\pm}$. A single or double dot between two pairs of vectors denotes a single or double contraction over the mode indices: $\mathbf{a}\cdot\mathbf{b} = \sum_{n=1}^{N_i} a_n b_n$, $\mathbf{ab}:\mathbf{cd} = \sum_{n=1}^{N_1}\sum_{m=1}^{N_2} a_n b_m c_m d_n$.

The pure state has density matrix $\Psi_{n\sigma,m\tau}\Psi^*_{n'\sigma',m'\tau'}$. By tracing over the detected modes the pure state is reduced to a mixed state with respect to the polarization degrees of freedom. The reduced density matrix is 4×4, with elements

$$\rho_{\sigma\tau,\sigma'\tau'} = \frac{1}{Z}\big(\mathbf{u}_{+\sigma}\mathbf{v}_{-\tau} + \mathbf{u}_{-\sigma}\mathbf{v}_{+\tau}\big) : \big(\mathbf{v}^*_{-\tau'}\mathbf{u}^*_{+\sigma'} + \mathbf{v}^*_{+\tau'}\mathbf{u}^*_{-\sigma'}\big), \tag{5.2}$$

$$Z = \sum_{\sigma,\tau}\big(\mathbf{u}_{+\sigma}\mathbf{v}_{-\tau} + \mathbf{u}_{-\sigma}\mathbf{v}_{+\tau}\big) : \big(\mathbf{v}^*_{-\tau}\mathbf{u}^*_{+\sigma} + \mathbf{v}^*_{+\tau}\mathbf{u}^*_{-\sigma}\big). \tag{5.3}$$

The complex numbers that enter into the density matrix are conveniently grouped into a pair of Hermitian positive definite matrices a and b, with elements $a_{\sigma\tau,\sigma'\tau'} = \mathbf{u}_{\sigma\tau}\cdot\mathbf{u}^*_{\sigma'\tau'}$, $b_{\sigma\tau,\sigma'\tau'} = \mathbf{v}_{\sigma\tau}\cdot\mathbf{v}^*_{\sigma'\tau'}$. One has

$$Z\rho_{\sigma\tau,\sigma'\tau'} = a_{+\sigma,+\sigma'}b_{-\tau,-\tau'} + a_{-\sigma,-\sigma'}b_{+\tau,+\tau'} + a_{-\sigma,+\sigma'}b_{+\tau,-\tau'} + a_{+\sigma,-\sigma'}b_{-\tau,+\tau'}. \tag{5.4}$$

The degree of entanglement of the mixed state with 4×4 density matrix ρ is quantified by the concurrence $\mathcal{C}$, given by [3]

$$\mathcal{C} = \max\left\{0, \sqrt{\lambda_1} - \sqrt{\lambda_2} - \sqrt{\lambda_3} - \sqrt{\lambda_4}\right\}. \tag{5.5}$$

The λ_i's are the eigenvalues of the matrix product

$$\rho\cdot(\sigma_y\otimes\sigma_y)\cdot\rho^*\cdot(\sigma_y\otimes\sigma_y),$$

in the order $\lambda_1 \geq \lambda_2 \geq \lambda_3 \geq \lambda_4$, with σ_y a Pauli matrix. The concurrence ranges from 0 (no entanglement) to 1 (maximal entanglement).

In a typical experiment [6], the photodetectors can not measure $\mathcal{C}$ directly, but instead infer the degree of entanglement through the maximal violation of the Bell-CHSH (Clauser-Horne-Shimony-Holt) inequality [4, 5]. The maximal value $\mathcal{E}_{\max}$ of the Bell-CHSH parameter for an arbitrary mixed state was analyzed in Refs. [7, 8]. For a pure state with concurrence $\mathcal{C}$ one has simply $\mathcal{E}_{\max} = 2\sqrt{1+\mathcal{C}^2}$ [9]. For a mixed state there is no one-to-one relation between $\mathcal{E}_{\max}$ and $\mathcal{C}$. Depending on the density matrix, $\mathcal{E}_{\max}$ can take on values between $2\mathcal{C}\sqrt{2}$ and $2\sqrt{1+\mathcal{C}^2}$, so $\mathcal{E}_{\max} > 2$ implies $\mathcal{C} > 0$ but not the other way around. The general formula

$$\mathcal{E}_{\max} = 2\sqrt{u_1+u_2} \tag{5.6}$$

for the dependence of $\mathcal{E}_{\max}$ on ρ involves the two largest eigenvalues u_1, u_2 of the real symmetric 3×3 matrix $R^{\mathrm{T}}R$ constructed from $R_{kl} = \mathrm{Tr}\,\rho\,\sigma_k \otimes \sigma_l$. Here $\sigma_1, \sigma_2, \sigma_3$ refer to the three Pauli matrices $\sigma_x, \sigma_y, \sigma_z$, respectively.

We will calculate both the true concurrence $\mathcal{C}$ and the pseudo-concurrence

$$\mathcal{C}' \equiv \sqrt{\max\left(0, \mathcal{E}_{\max}^2/4 - 1\right)} \leq \mathcal{C} \tag{5.7}$$

inferred from the Bell inequality violation.

As a special case we will also consider what happens if only one of the two beams is scattered. The other beam reaches the photodetector without changing its mode or polarization, so we set $v^{\pm}_{m\sigma} = \delta_{m,1}\delta_{\sigma,\pm}$. This implies $b_{\sigma\tau,\sigma'\tau'} = \delta_{\sigma,\tau}\delta_{\sigma',\tau'}$, hence

$$Z\rho_{\sigma\tau,\sigma'\tau'} = a_{\bar{\tau}\sigma,\bar{\tau}'\sigma'}, \tag{5.8}$$

where we have defined $\bar{\tau} = -\tau$. The normalization is now given simply by $Z = \sum_{\sigma,\tau} a_{\sigma\tau,\sigma\tau}$.

5.3 Random-matrix theory

For a statistical description we use results from the random-matrix theory (RMT) of scattering by disordered media [1, 2]. According to that theory, the real and imaginary parts of the complex scattering amplitudes $u^{\sigma}_{n\tau}$ are statistically distributed as independent random variables with the same Gaussian distribution of zero mean. The variance of the Gaussian drops out of the density matrix; we fix it at 1. The assumption of independent variables ignores the orthonormality constraint of the vectors u, which is justified if $N_1 \ll M_1$. Similarly, for $N_2 \ll M_2$ the real and imaginary parts of $v^{\sigma}_{n\tau}$ have independent Gaussian distributions with zero mean and a variance which we may set at 1.

The reduced density matrix of the mixed state depends on the two independent random matrices a and b, according to Eq. (5.4). The matrix elements are not independent. We calculate the joint probability distribution of the matrix elements, using the following result from RMT [10]: Let W be a rectangular matrix of dimension $p \times (k+p)$, filled with complex numbers with distribution

$$P(\{W_{nm}\}) \propto \exp\left(-c \operatorname{Tr} W W^\dagger\right), \quad c > 0. \tag{5.9}$$

Then the square matrix $H = WW^\dagger$ (of dimension $p \times p$) has the Laguerre distribution

$$P(\{H_{nm}\}) \propto (\operatorname{Det} H)^k \exp(-c \operatorname{Tr} H). \tag{5.10}$$

Note that H is Hermitian and positive definite, so its eigenvalues h_n ($n = 1, 2, \ldots p$) are real positive numbers. Their joint distribution is that of the Laguerre unitary ensemble,

$$P(\{h_n\}) \propto \prod_n h_n^k e^{-ch_n} \prod_{i<j} (h_i - h_j)^2. \tag{5.11}$$

The factor $(h_i - h_j)^2$ is the Jacobian of the transformation from complex matrix elements to real eigenvalues. The eigenvectors of H form a unitary matrix U which is uniformly distributed in the unitary group.

To apply this to the matrix a we set $c = 1/2$, $p = 4$, $k = N_1 - 4$. We first assume that $N_1 \geq 4$, to ensure that $k \geq 0$. Then

$$P(\{a_{\sigma\tau,\sigma'\tau'}\}) \propto (\operatorname{Det} a)^{N_1-4} \exp\left(-\tfrac{1}{2} \operatorname{Tr} a\right), \tag{5.12}$$

$$P(\{a_n\}) \propto \prod_n a_n^{N_1-4} e^{-a_n/2} \prod_{i<j} (a_i - a_j)^2, \tag{5.13}$$

where a_1, a_2, a_3, a_4 are the real positive eigenvalues of a. The 4×4 matrix U of eigenvectors of a is uniformly distributed in the unitary group. If $N_1 = 1, 2, 3$ we set $c = 1/2$, $p = N_1$, $k = 4 - N_1$. The matrix a has $4 - N_1$ eigenvalues equal to 0. The N_1 non-zero eigenvalues have distribution

$$P(\{a_n\}) \propto \prod_n a_n^{4-N_1} e^{-a_n/2} \prod_{i<j} (a_i - a_j)^2. \tag{5.14}$$

The distribution of the matrix elements $b_{\sigma\tau,\sigma'\tau'}$ and of the eigenvalues b_n is obtained upon replacement of N_1 by N_2 in Eqs. (5.12), (5.13), and (5.14).

5.4 Asymptotic analysis

We wish to average the concurrence (5.5) and pseudo-concurrence (5.7) with the RMT distribution of Sec. 5.3. The result depends only on the number of detected modes N_1, N_2 in the two photodetectors. Microscopic details of the scattering media become irrelevant once we assume random scattering. The averages $\langle \mathcal{C} \rangle$, $\langle \mathcal{C}' \rangle$ can be calculated by numerical integration [11]. Before presenting these results, we analyze the asymptotic behavior for $N_i \gg 1$ analytically. We assume for simplicity that $N_1 = N_2 \equiv N$.

It is convenient to scale the eigenvalues as

$$a_n = 2N(1+\alpha_n), \;\; b_n = 2N(1+\beta_n). \tag{5.15}$$

The distribution of the α_n's and β_n's takes the same form

$$P(\{\alpha_n\}) \propto \exp\left(-N \sum_{n=1}^{4} [\alpha_n - \ln(1+\alpha_n)] + \mathcal{O}(1) \right), \tag{5.16}$$

where $\mathcal{O}(1)$ denotes N-independent terms. The bulk of the distribution (5.16) lies in the region $\sum_n \alpha_n^2 \lesssim 1/N \ll 1$, localized at the origin. Outside of this region the distribution decays exponentially $\propto \exp[-Nf(\{\alpha_n\})]$, with

$$f(\{\alpha_n\}) = \sum_{n=1}^{4} [\alpha_n - \ln(1+\alpha_n)]. \tag{5.17}$$

The concurrence $\mathcal{C}$ and pseudo-concurrence $\mathcal{C}'$ depend on the rescaled eigenvalues α_n, β_n and also on the pair of 4×4 unitary matrices U, V of eigenvectors of a and b. Both quantities are *independent* of N, because the scale factor N in Eq. (5.15) drops out of the density matrix (5.4) upon normalization.

The two quantities $\mathcal{C}$ and $\mathcal{C}'$ are identically zero when the α_n's and β_n's are all $\ll 1$ in absolute value. For a nonzero value one has to go deep into the tail of the eigenvalue distribution. The average of $\mathcal{C}$ is dominated by the "optimal fluctuation" $\alpha_n^{\rm opt}$, $\beta_n^{\rm opt}$, $U^{\rm opt}$, $V^{\rm opt}$ of eigenvalues and eigenvectors, which minimizes $f(\{\alpha_n\}) + f(\{\beta_n\})$ in the region $\mathcal{C} > 0$. The decay

$$\langle \mathcal{C} \rangle \simeq \exp\left(-N[f(\{\alpha_n^{\rm opt}\}) + f(\{\beta_n^{\rm opt}\})] \right) \equiv e^{-AN} \tag{5.18}$$

of the average concurrence is exponential in N, with a coefficient A of order unity determined by the optimal fluctuation. The average $\langle \mathcal{C}' \rangle \simeq e^{-BN}$ also decays exponentially with N, but with a different coefficient B in the exponent. The

numbers A and B can be calculated analytically for the case that only one of the two beams is scattered.

Scattering of a single beam corresponds to a density matrix ρ which is directly given by the matrix a, cf. Eq. (5.8). To find A, we therefore need to minimize $f(\{\alpha_n\})$ over the eigenvalues and eigenvectors of a with the constraint $\mathcal{C} > 0$,

$$A = \min_{\{\alpha_n\},U} \left\{ f(\{\alpha_n\}) | \, \mathcal{C}\big(\rho(\{\alpha_n\},U)\big) > 0 \right\}. \tag{5.19}$$

The minimum can be found with the help of the following result [12]: The concurrence $\mathcal{C}(\rho)$ of the two-qubit density matrix ρ, with fixed eigenvalues $\Lambda_1 \geq \Lambda_2 \geq \Lambda_3 \geq \Lambda_4$ but arbitrary eigenvectors, is maximized upon unitary transformation by

$$\max_{\Omega} \mathcal{C}(\Omega\,\rho\,\Omega^\dagger) = \max\left\{0, \Lambda_1 - \Lambda_3 - 2\sqrt{\Lambda_2\Lambda_4}\right\}. \tag{5.20}$$

(The matrix Ω varies over all 4×4 unitary matrices.) With this knowledge, Eq. (5.19) reduces to

$$A = \min_{\{\alpha_n\}} \left\{ f(\{\alpha_n\}) | \alpha_1 - \alpha_3 - 2\sqrt{(1+\alpha_2)(1+\alpha_4)} > 0 \right\}, \tag{5.21}$$

where we have ordered $\alpha_1 \geq \alpha_2 \geq \alpha_3 \geq \alpha_4$. This yields for the optimal fluctuation $\alpha_1^{\rm opt} = 1$, $\alpha_2^{\rm opt} = \alpha_3^{\rm opt} = \alpha_4^{\rm opt} = -1/3$ and

$$A = 3\ln 3 - 4\ln 2 = 0.523. \tag{5.22}$$

The asymptotic decay $\langle \mathcal{C} \rangle \propto e^{-AN}$ is in good agreement with a numerical calculation for finite N, see Fig. 5.2.

The asymptotic decay of the average pseudo-concurrence $\langle \mathcal{C}' \rangle$ for a single scattered beam can be found in a similar way, using the result [8]

$$\max_{\Omega} \mathcal{C}'(\Omega\,\rho\,\Omega^\dagger) = \sqrt{\max\left\{0, 2(\Lambda_1-\Lambda_4)^2 + 2(\Lambda_2-\Lambda_3)^2 - (\Lambda_1+\Lambda_2+\Lambda_3+\Lambda_4)^2\right\}}. \tag{5.23}$$

To obtain the optimal fluctuation we have to solve

$$B = \min_{\{\alpha_n\}} \left\{ f(\{\alpha_n\}) | 2(\alpha_1-\alpha_4)^2 + 2(\alpha_2-\alpha_3)^2 - (4+\alpha_1+\alpha_2+\alpha_3+\alpha_4)^2 > 0 \right\}, \tag{5.24}$$

which gives

$$\alpha_1^{\rm opt} = \frac{1}{2}(-1+2\sqrt{2}+\sqrt{5}),\ \alpha_2^{\rm opt} = \alpha_3^{\rm opt} = \frac{1}{2}(1-\sqrt{5}),\ \alpha_4^{\rm opt} = \frac{1}{2}(-1-2\sqrt{2}+\sqrt{5}), \tag{5.25}$$

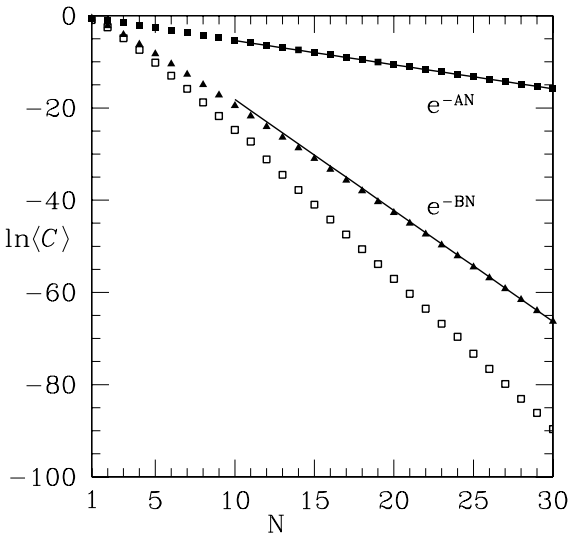

Figure 5.2: Average concurrence $\langle \mathcal{C} \rangle$ (squares) and pseudo-concurrence $\langle \mathcal{C}' \rangle$ (triangles) as a function of the number N of detected modes. Closed symbols are for the case that only one of the two beams is scattered and open symbols for the case that both beams are scattered. The decay of $\langle \mathcal{C}' \rangle$ in the latter case could not be determined accurately enough and is therefore omitted from the plot. The solid lines are the analytically obtained exponential decays, with constants $A = 3\ln 3 - 4\ln 2$ and $B = \ln(11 + 5\sqrt{5}) - \ln 2$, cf. Eqs. (5.22) and (5.26).

hence

$$B = \ln(11 + 5\sqrt{5}) - \ln 2 = 2.406. \tag{5.26}$$

The decay $\langle \mathcal{C}' \rangle \propto e^{-BN}$ is again in good agreement with the numerical results for finite N (Fig. 5.2).

If both beams are scattered, a calculation of the optimal fluctuation is more complicated because the eigenvalues $\{\alpha_n\}$, $\{\beta_n\}$ and the eigenvectors U, V get mixed in the density matrix (5.4). The numerics of Fig. 5.2 gives $\langle \mathcal{C} \rangle \propto e^{-3.3N}$ for the asymptotic decay of the concurrence. The averaged pseudo-concurrence for two-beam scattering could not be determined accurately enough to extract a reliable value for the decay constant.

5.5 Polarization-conserving scattering

If the scatterers are translationally invariant in one direction, then the two polarizations are not mixed by the scattering. Such scatterers have been realized as parallel glass fibers [13]. One polarization corresponds to the electric field parallel to the scatterers (TE polarization), the other to parallel magnetic field (TM polarization). The boundary condition differs for the two polarizations (Dirichlet for TE and Neumann for TM), so the scattering amplitudes $\mathbf{u}_{++}$, $\mathbf{v}_{++}$, $\mathbf{u}_{--}$, $\mathbf{v}_{--}$ that conserve the polarization can still be considered to be independent random numbers. The amplitudes that couple different polarizations vanish: $\mathbf{u}_{+-}$, $\mathbf{v}_{+-}$, $\mathbf{u}_{-+}$, $\mathbf{v}_{-+}$ are all zero.

The reduced density matrix (5.4) simplifies to

$$Z\rho_{\sigma\tau,\sigma'\tau'} = \delta_{\sigma,\bar{\tau}}\delta_{\sigma',\bar{\tau}'}a_{\sigma\sigma,\sigma'\sigma'}b_{\tau\tau,\tau'\tau'}, \tag{5.27}$$

with $\bar{\tau} = -\tau$, $\bar{\tau}' = -\tau'$. We will abbreviate $A_{\sigma\tau} \equiv a_{\sigma\sigma,\tau\tau}$, $B_{\sigma\tau} \equiv b_{\sigma\sigma,\tau\tau}$. The concurrence $\mathcal{C}$ and pseudo-concurrence $\mathcal{C}'$ are calculated from Eqs. (5.5) and (5.7), with the result

$$\mathcal{C} = \mathcal{C}' = \frac{2|A_{+-}||B_{+-}|}{A_{++}B_{--} + A_{--}B_{++}}. \tag{5.28}$$

It is again our objective to calculate $\langle\mathcal{C}\rangle$ for the case $N_1 = N_2 = N$. The distribution of the matrices A and B follows by substituting $N_1 - 4 \to N - 2$ in Eq. (5.12):

$$P(\{A_{\sigma\tau}\}) \propto (\mathrm{Det}\, A)^{N-2} \exp\left(-\tfrac{1}{2}\mathrm{Tr}\, A\right). \tag{5.29}$$

The average over this distribution was done numerically, see Fig. 5.3. For large N we may perform the following asymptotic analysis.

We scale the matrices A and B as

$$A = 2N(\mathbb{1} + \mathcal{A}), \quad B = 2N(\mathbb{1} + \mathcal{B}). \tag{5.30}$$

In the limit $N \to \infty$ the Hermitian matrices $\mathcal{A}$ and $\mathcal{B}$ have the Gaussian distribution

$$P(\{\mathcal{A}_{\sigma\tau}\}) \propto e^{-\frac{1}{2}N\mathrm{Tr}\mathcal{A}\mathcal{A}^\dagger}. \tag{5.31}$$

(The same distribution holds for $\mathcal{B}$.) In contrast to the analysis in Sec. 5.4 the concurrence does not vanish in the bulk of the distribution. The average of Eq. (5.28) with distribution (5.31) yields the algebraic decay

$$\langle\mathcal{C}\rangle = \frac{\pi}{4}\frac{1}{N}, \quad N \gg 1, \tag{5.32}$$

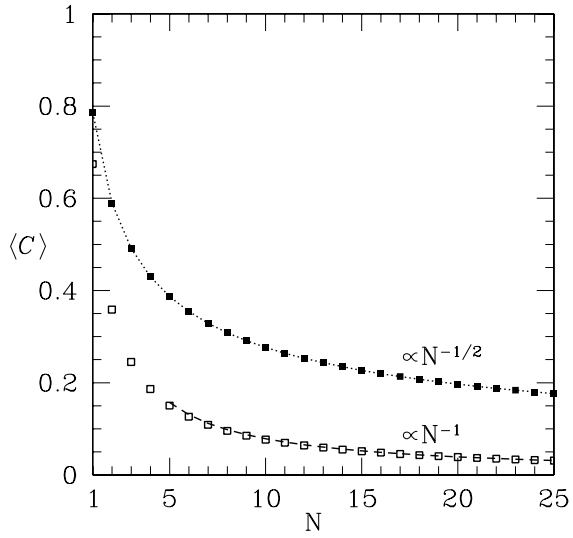

Figure 5.3: Average concurrence $\langle \mathcal{C} \rangle$ as a function of the number N of detected modes, for the case of polarization-conserving scattering of both beams (open squares) and one beam (closed squares). The data points are the result of a numerical average. The dashed line is the asymptotic result (5.32) and the dotted line is the analytical result (5.34). The pseudo-concurrence $\mathcal{C}'$ is identical to $\mathcal{C}$ for polarization-conserving scattering.

in good agreement with the numerical calculation for finite N (Fig. 5.3).

A completely analytical calculation for any N can be done in the case that only one of the beams is scattered. In that case $B_{\sigma\tau} = 1$ and the concurrence reduces to

$$\mathcal{C} = \frac{2|A_{+-}|}{A_{++} + A_{--}}. \tag{5.33}$$

Averaging Eq. (5.33) over the Laguerre distribution (5.29) gives

$$\langle \mathcal{C} \rangle = \frac{\sqrt{\pi}}{2} \frac{\Gamma(N+1/2)}{\Gamma(N+1)}. \tag{5.34}$$

For large N, the average concurrence (5.34) falls off as

$$\langle \mathcal{C} \rangle = \frac{\sqrt{\pi}}{2} \frac{1}{\sqrt{N}}, \quad N \gg 1. \tag{5.35}$$

This case is also included in Fig. 5.3.

5.6 Conclusion

In summary, we have applied the method of random-matrix theory (RMT) to the problem of entanglement transfer through a random medium. RMT has been used before to study *production* of entanglement [14–21]. Here we have studied the *loss* of entanglement in the transition from a pure state to a mixed state.

A common feature of all these theories is that the results are universal, independent of microscopic details. In our problem the decay of the degree of entanglement depends on the number of detected modes but not on microscopic parameters such as the scattering mean free path.

The origin of this universality is the central limit theorem: The complex scattering amplitude from one mode in the source to one mode in the detector is the sum over a large number of complex partial amplitudes, corresponding to different sequences of multiple scattering. The probability distribution of the sum becomes a Gaussian with zero mean (because the random phases of the partial amplitudes average out to zero). The variance of the Gaussian will depend on the mean free path, but it drops out upon normalization of the reduced density matrix. The applicability of the central limit theorem only requires that the scattering medium is thick compared to the mean free path, to ensure a large number of terms in the sum over partial amplitudes.

The degree of entanglement (as quantified by the concurrence or violation of the Bell inequality) then depends only on the number N of detected modes.

We have identified two qualitatively different types of decay. The decay is exponential $\propto e^{-cN}$ if the scattering mixes spatial modes as well as polarization directions. The coefficient c depends on which measure of entanglement one uses (concurrence or violation of Bell inequality) and it also depends on whether both photons in the Bell pair are scattered or only one of them is. For this latter case of single-beam scattering, the coefficients c are $3\ln 3 - 4\ln 2$ (concurrence) and $\ln(11+5\sqrt{5}) - \ln 2$ (pseudo-concurrence). The decay is algebraic $\propto N^{-p}$ if the scattering preserves the polarization. The power p is 1 if both photons are scattered and $1/2$ if only one of them is. Polarization-conserving scattering is special; it would require translational invariance of the scatterers in one direction. The generic decay is therefore exponential.

Finally, we remark that the results presented here apply not only to scattering by disorder, but also to scattering by a cavity with a chaotic phase space. An experimental search for entanglement loss by chaotic scattering has been reported by Woerdman *et al.* [22].

Bibliography

[1] C. W. J. Beenakker, Rev. Mod. Phys. **69**, 731 (1997).

[2] T. Guhr, A. Müller-Groeling, and H. A. Weidenmüller, Phys. Rep. **299**, 189 (1998).

[3] W. K. Wootters, Phys. Rev. Lett. **80**, 2245 (1998).

[4] J. S. Bell, Physics **1**, 195 (1964).

[5] J. F. Clauser, M. A. Horne, A. Shimony, and R. A. Holt, Phys. Rev. Lett. **23**, 880 (1969).

[6] E. Altewischer, M. P. van Exter, and J. P. Woerdman, Nature **418**, 304 (2002).

[7] R. Horodecki, P. Horodecki, and M. Horodecki, Phys. Lett. A **200**, 340 (1995).

[8] F. Verstraete and M. M. Wolf, Phys. Rev. Lett. **89**, 170401 (2002).

[9] N. Gisin, Phys. Lett. A **154**, 201 (1991).

[10] J. Verbaarschot, Nucl. Phys. B **426**, 559 (1994).

[11] The results of Fig. 5.2 are obtained by a combination of adaptive integration over the simplex of eigenvalues $\{a_n\}$ (and $\{b_n\}$) and a stochastic average over the unitary matrix U (and V). We define the scaled eigenvalues $\{\tilde{a}_n\}$ by $a_2 = a_1\tilde{a}_2$, $a_3 = a_1\tilde{a}_2\tilde{a}_3$, $a_4 = a_1\tilde{a}_2\tilde{a}_3\tilde{a}_4$, and similarly for $\{\tilde{b}_n\}$. The eigenvalues a_1 (and b_1) are then integrated out analytically. This can be done since ρ (and hence $\mathcal{C}$ and $\mathcal{C}'$) is left invariant upon scaling $\{a_n\}$ and $\{b_n\}$. In the case that one beam is scattered, we averaged over 4000 random unitary matrices U and used a maximum of 6000 integration points in the cube of scaled

eigenvalues ($0 \leq \tilde{a}_n \leq 1, n = 2,3,4$). For scattering of both beams, an average over 1000 pairs of U and V was taken with a maximum of $12 \cdot 10^5$ points in the 6-dimensional space of combined cubes.

[12] F. Verstraete, K. Audenaert, and B. De Moor, Phys. Rev. A **64**, 012316 (2001).

[13] E. A. Montie, E. C. Cosman, G. W. 't Hooft, M. B. van der Mark, and C. W. J. Beenakker, Nature **350**, 594 (1991).

[14] K. Furuya, M. C. Nemes, and G. Q. Pellegrino, Phys. Rev. Lett. **80**, 5524 (1998).

[15] P. A. Miller and S. Sarkar, Phys. Rev. E **60**, 1542 (1999).

[16] K. Życzkowski and H.-J. Sommers, J. Phys. A **34**, 7111 (2001).

[17] J. N. Bandyopadhyay and A. Lakshminarayan, Phys. Rev. Lett. **89**, 060402 (2002).

[18] M. Žnidarič and T. Prosen, J. Phys. A **36**, 2463 (2003).

[19] A. J. Scott and C. M. Caves, J. Phys. A **36**, 9553 (2003).

[20] Ph. Jacquod, Phys. Rev. Lett. **92**, 150403 (2004).

[21] C. W. J. Beenakker, M. Kindermann, C. M. Marcus, and A. Yacoby, in *Fundamental Problems of Mesoscopic Physics*, edited by I. V. Lerner, B.L. Altshuler, and Y. Gefen, NATO Science Series II. Vol. 154 (Kluwer, Dordrecht, 2004).

[22] J. P. Woerdman, talk presented at the workshop "Fundamentals of Solid State Quantum Information Processing", Lorentz Center, Leiden University (2003).

Chapter 6

Entangling ability of a beam splitter in the presence of temporal which-path information

6.1 Introduction

Entanglement, the nonclassical correlations between spatially separated particles, is typically a signature of interactions in the past or emergence from a common source. However, it can also arise as the interference of identical particles [1]. By postselecting experimental data based on the "click" of detectors [2, 3], photons scattered at a beam splitter have violated a Bell inequality, even if they originated from independent sources [4, 5]. In reverse, triggered by an interferometric Bell-state measurement, entanglement has been swapped [6] to initially uncorrelated photons of different Bell pairs [7–9]. The observation of these nonclassical interference effects is an important step on the road towards an optical approach of quantum information processing [10, 11].

Being furnished by interference, the ability of a beam splitter to entangle the polarizations of two independent photons depends on their indistinguishability [12]. One of the incident photons is horizontally polarized in state $|\mathrm{H};\psi\rangle$, the other vertically polarized in $|\mathrm{V};\phi\rangle$. The photons are partially distinguishable by their temporal degrees of freedom captured in the kets $|\psi\rangle$ and $|\phi\rangle$. Besides temporal which-path information inherited from incident photons, a scattered two-photon state possibly holds polarization which-path information. We make no assumptions about the scattering amplitudes connecting polarizations at the beam splitter, except that they constitute a unitary scattering matrix. Trans-

lated to a polarization-conserving beam splitter, this corresponds to incident photons in states $|\sigma;\psi\rangle$ and $|\sigma';\phi\rangle$ where σ, σ' are arbitrary superpositions of H, V. The analysis presented in this chapter generalizes existing work on a polarization-conserving beam splitter where $\sigma = \mathrm{H}$ and $\sigma' = \mathrm{V}$ [5, 13].

The polarization-state ρ of a scattered photon pair is established from the scattering amplitudes of the beam splitter, the shape and timing of photonic wavepackets ($|\psi\rangle$, $|\phi\rangle$) and the time-window of coincidence detection. If not erased by ultra-coincidence detection, an amount of temporal distinguishability of $(1 - |\langle\psi|\phi\rangle|^2)$ pertains corresponding to a mixed state ρ. We calculate both its concurrence and the Bell-CHSH parameter. The ability of the latter to witness entanglement can disappear in the presence of a Mandel dip. In terms of a polarization-conserving beam splitter, this corresponds to a deviation of σ, σ' from $\sigma = \mathrm{H}$ and $\sigma' = \mathrm{V}$.

6.2 Formulation of the problem

In a second-quantized notation, the incident two-photon state $|\mathrm{H};\psi\rangle_\mathrm{L}|\mathrm{V};\phi\rangle_\mathrm{R}$ takes the form

$$|\Psi_\mathrm{in}\rangle = \Psi^\dagger_\mathrm{H,L}\Phi^\dagger_\mathrm{V,R}|0\rangle, \tag{6.1}$$

with field creation operators given by (see Fig. 6.1)

$$\Psi^\dagger_\mathrm{H,L} = \int d\omega\, a^\dagger_\mathrm{H}(\omega)\psi^*(\omega), \quad \Phi^\dagger_\mathrm{V,R} = \int d\omega\, b^\dagger_\mathrm{V}(\omega)\phi^*(\omega). \tag{6.2}$$

(The subscripts R,L indicate the two sides of the beam splitter.) The operators $a_i(\omega)$ with $i = \mathrm{H},\mathrm{V}$ satisfy commutation rules

$$[a_i(\omega), a_j(\omega')] = 0, \quad [a_i(\omega), a^\dagger_j(\omega')] = \delta_{ij}\delta(\omega - \omega'). \tag{6.3}$$

The same commutation rules hold for the operators $b_i(\omega)$, with commutation among a and b.

The outgoing operators $c_i(\omega)$, $d_i(\omega)$ are related to the incoming ones $a_i(\omega)$, $b_i(\omega)$ by a 4×4 unitary scattering matrix S, decomposed in 2×2 reflection and transmission matrices r,t,t',r':

$$\begin{pmatrix} c(\omega) \\ d(\omega) \end{pmatrix} = \begin{pmatrix} r & t' \\ t & r' \end{pmatrix}\begin{pmatrix} a(\omega) \\ b(\omega) \end{pmatrix}, \quad a(\omega) \equiv \begin{pmatrix} a_\mathrm{H}(\omega) \\ a_\mathrm{V}(\omega) \end{pmatrix}, \tag{6.4}$$

and vectors $b(\omega)$, $c(\omega)$, $d(\omega)$ defined similarly. The scattering amplitudes are frequency-independent. The outgoing state $|\Psi_\mathrm{out}\rangle$ can be conveniently written in

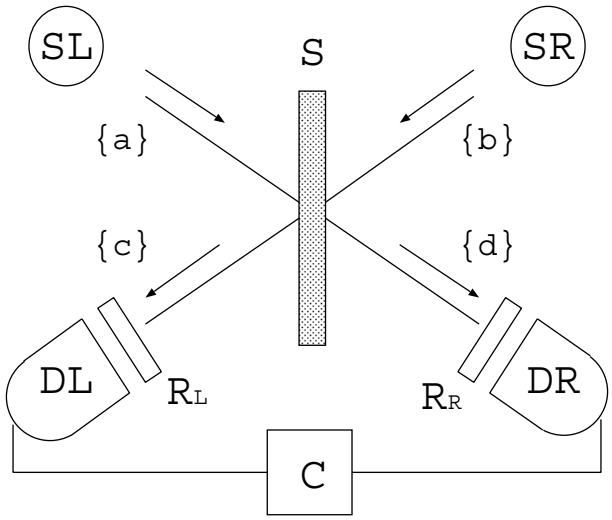

Figure 6.1: Schematic drawing of generation and detection of polarization-entanglement at a beam splitter. The independent sources SL and SR each create a photon in modes $\{a\}$ and $\{b\}$ cf. Eq. (6.1). The beam splitter with unitary 4×4 scattering matrix S couples the polarization of incoming modes to the polarization of outgoing modes $\{c\}$ and $\{d\}$. Polarizations are locally mixed by R_{L} and R_{R}. A coincidence circuit C registers simultaneous detection of photons by photodetectors DL and DR.

a matrix notation

$$|\Psi_{\mathrm{out}}\rangle = \int d\omega \int d\omega'\, \psi^*(\omega)\phi^*(\omega') \begin{pmatrix} c^\dagger(\omega) \\ d^\dagger(\omega) \end{pmatrix}^{\mathrm{T}} \begin{pmatrix} r\sigma_{\mathrm{in}}t'^{\mathrm{T}} & r\sigma_{\mathrm{in}}r'^{\mathrm{T}} \\ t\sigma_{\mathrm{in}}t'^{\mathrm{T}} & t\sigma_{\mathrm{in}}r'^{\mathrm{T}} \end{pmatrix} \begin{pmatrix} c^\dagger(\omega') \\ d^\dagger(\omega') \end{pmatrix} |0\rangle. \tag{6.5}$$

Here we used the unitarity of S and $\sigma_{\mathrm{in}} = (\sigma_x + i\sigma_y)/2$, with σ_x and σ_y Pauli matrices, corresponds to the polarizations of the incoming photons cf. Eq. (6.1). The matrix σ_{in} has rank 1 reflecting the fact that polarizations are not entangled prior to scattering. Since we make no assumptions about the scattering amplitudes (apart from the unitarity of S), the choice of σ_{in} is without loss of generality (see Appendix 6.A).

The joint probability per unit (time)^2 of absorbing a photon with polarization i at detector DL and a photon with polarization j at detector DR at times t and t'

respectively is given by [14]

$$w_{ij}(t,t') \propto \langle \Psi_{\rm out}| E^{(-)}_{i\rm L}(t) E^{(-)}_{j\rm R}(t') E^{(+)}_{j\rm R}(t') E^{(+)}_{i\rm L}(t) |\Psi_{\rm out}\rangle, \tag{6.6}$$

where $E^{(+)}_{i\rm L}(t)$ and $E^{(+)}_{i\rm R}(t)$ are the positive frequency field operators of polarization i at detectors DL and DR. The probability $C_{ij}(t)$ of a coincidence event within time-windows τ around t is given by

$$C_{ij}(t) = \int_{t-\frac{\tau}{2}}^{t+\frac{\tau}{2}} dt' \int_{t-\frac{\tau}{2}}^{t+\frac{\tau}{2}} dt'' w_{ij}(t',t''). \tag{6.7}$$

Experimentally, the time-window τ has typically a lower bound determined by the random rise time of an avalanche of charge carriers in response to a photon absorption event.

The polarization-entanglement is detected by violation of the Bell-CHSH inequality [15]. This requires two local polarization mixers $R_{\rm L}$ and $R_{\rm R}$. The Bell-CHSH parameter $\mathcal{E}$ is

$$\mathcal{E} = |E(R_{\rm L}, R_{\rm R}) + E(R'_{\rm L}, R_{\rm R}) + E(R_{\rm L}, R'_{\rm R}) - E(R'_{\rm L}, R'_{\rm R})|, \tag{6.8}$$

where $E(R_{\rm L}, R_{\rm R})$ is related to the correlators $C_{ij}(R_{\rm L}, R_{\rm R})$ by

$$E = \frac{C_{\rm HH} + C_{\rm VV} - C_{\rm HV} - C_{\rm VH}}{C_{\rm HH} + C_{\rm VV} + C_{\rm HV} + C_{\rm VH}}. \tag{6.9}$$

Substituting the correlators of Eq. (6.7) into Eq. (6.9), we see that

$$E(R_{\rm L}, R_{\rm R}) = {\rm Tr}\, \rho\, (R^\dagger_{\rm L} \sigma_z R_{\rm L}) \otimes (R^\dagger_{\rm R} \sigma_z R_{\rm R}), \tag{6.10}$$

where σ_z is a Pauli matrix and ρ a 4×4 polarization density matrix with elements

$$\rho_{ij,mn} = \frac{1}{\mathcal{N}} \left((1+|\alpha|^2)(\gamma_1)_{ij}(\gamma_1)^*_{mn} + (1-|\alpha|^2)(\gamma_2)_{ij}(\gamma_2)^*_{mn} \right). \tag{6.11}$$

The parameter α is given by

$$\begin{aligned} \alpha \;=\; & \left(\int_{t-\frac{\tau}{2}}^{t+\frac{\tau}{2}} dt' \int d\omega \int d\omega' \phi(\omega) \psi^*(\omega') e^{i(\omega-\omega')t'} \right) \;\times \\ & \left(\int_{t-\frac{\tau}{2}}^{t+\frac{\tau}{2}} dt' \int d\omega \int d\omega' \phi(\omega) \phi^*(\omega') e^{i(\omega-\omega')t'} \right)^{-1/2} \times \\ & \left(\int_{t-\frac{\tau}{2}}^{t+\frac{\tau}{2}} dt' \int d\omega \int d\omega' \psi(\omega) \psi^*(\omega') e^{i(\omega-\omega')t'} \right)^{-1/2} \end{aligned} \tag{6.12}$$

and γ_1,γ_2 are 2×2 matrices related to the scattering amplitudes by

$$\gamma_1 = r\sigma_{\rm in} r'^{\rm T} + t'\sigma_{\rm in}^{\rm T} t^{\rm T}, \quad \gamma_2 = r\sigma_{\rm in} r'^{\rm T} - t'\sigma_{\rm in}^{\rm T} t^{\rm T}. \tag{6.13}$$

The normalization factor $\mathcal{N}$ takes the form

$$\mathcal{N} = (1+|\alpha|^2){\rm Tr}\,\gamma_1^\dagger\gamma_1 + (1-|\alpha|^2){\rm Tr}\,\gamma_2^\dagger\gamma_2. \tag{6.14}$$

The parameter $1-|\alpha|^2 \in (0,1)$ represents the amount of temporal which-path information. Generally, the time-window τ is much larger than the coherence times or temporal difference of the wavepackets. We may then take the limit $\tau\to\infty$ and α reduces to the overlap of wavepackets

$$\alpha = \int d\omega\phi(\omega)\psi^*(\omega). \tag{6.15}$$

In the opposite limit of ultra-coincidence detection where $\tau\to 0$, temporal which-path information is completely erased corresponding to $|\alpha|^2 = 1$.

6.3 Entanglement of formation

The entanglement of formation of the mixed state ρ is quantified by the concurrence $\mathcal{C}$ [16] given by

$$\mathcal{C} = \max\left(0, \sqrt{\lambda_1} - \sqrt{\lambda_2} - \sqrt{\lambda_3} - \sqrt{\lambda_4}\right). \tag{6.16}$$

The λ_i's are the eigenvalues of the matrix product $\rho\tilde{\rho}$, where $\tilde{\rho} = (\sigma_y\otimes\sigma_y)\rho^*(\sigma_y\otimes\sigma_y)$, in the order $\lambda_1\geq\lambda_2\geq\lambda_3\geq\lambda_4$. The concurrence ranges from 0 (no entanglement) to 1 (maximal entanglement). For simplicity of notation it is convenient to define $(\widehat{xy})_{ij,mn} \equiv x_{ij}y^*_{mn}$. The matrix $\tilde{\rho}$ can be written as

$$\tilde{\rho} = \frac{1}{\mathcal{N}}\left((1+|\alpha|^2)\widehat{\tilde{\gamma}_1\tilde{\gamma}_1} + (1-|\alpha|^2)\widehat{\tilde{\gamma}_2\tilde{\gamma}_2}\right), \tag{6.17}$$

with $\tilde{\gamma} \equiv \sigma_y\gamma^*\sigma_y$. The product $\rho\tilde{\rho}$ takes the simple form

$$\rho\tilde{\rho} = \frac{{\rm Tr}\,\gamma_1^\dagger\tilde{\gamma}_1}{\mathcal{N}^2}\left((1+|\alpha|^2)^2\widehat{\gamma_1\tilde{\gamma}_1} - (1-|\alpha|^2)^2\widehat{\gamma_2\tilde{\gamma}_2}\right), \tag{6.18}$$

where we have used the multiplication rule $\widehat{xy}\widehat{vw} = ({\rm Tr}\,y^\dagger v)\widehat{xw}$ and

$${\rm Tr}\,\gamma_1^\dagger\tilde{\gamma}_1 = -{\rm Tr}\,\gamma_2^\dagger\tilde{\gamma}_2, \quad {\rm Tr}\,\gamma_1^\dagger\tilde{\gamma}_2 = {\rm Tr}\,\gamma_2^\dagger\tilde{\gamma}_1 = 0. \tag{6.19}$$

The results for the tilde inner products of Eq. (6.19) hold since the photons are not polarization-entangled prior to scattering ($\mathrm{Det}\,\sigma_{\mathrm{in}} = 0$).

The non-Hermitian matrix $\rho\tilde{\rho}$ has eigenvalue-eigenvector decomposition

$$\rho\tilde{\rho} = \frac{|\mathrm{Tr}\,\gamma_1^\dagger\tilde{\gamma}_1|^2}{\mathcal{N}^2}\left(\sum_{i=1,2}\widehat{\gamma_i s_i}\right)\left((1+|\alpha|^2)^2\widehat{s_1 s_1}+(1-|\alpha|^2)^2\widehat{s_2 s_2}\right)\left(\sum_{i=1,2}\widehat{\gamma_i s_i}\right)^{-1}, \tag{6.20}$$

where we have defined orthonormal states $s_1 = (1/2)(\mathbb{1}+\sigma_z)$ and $s_2 = (1/2)(\sigma_x + i\sigma_y)$. The pseudo-inverse is easily seen to be

$$\left(\sum_{i=1,2}\widehat{\gamma_i s_i}\right)^{-1} = \frac{1}{(\mathrm{Tr}\,\gamma_1^\dagger\tilde{\gamma}_1)^*}\left(\widehat{s_1\tilde{\gamma}_1}-\widehat{s_2\tilde{\gamma}_2}\right). \tag{6.21}$$

It follows that

$$\mathcal{C} = \frac{2|\alpha|^2|\mathrm{Tr}\,\gamma_1^\dagger\tilde{\gamma}_1|}{\mathcal{N}}. \tag{6.22}$$

The trace that appears in the numerator of Eq. (6.22) is given by

$$|\mathrm{Tr}\,\gamma_1^\dagger\tilde{\gamma}_1| = 2\sqrt{\mathrm{Det}\,X^\dagger X\,\mathrm{Det}(\mathbb{1}-X^\dagger X)}, \tag{6.23}$$

where we have defined a "hybrid" 2×2 matrix

$$X = \begin{pmatrix} r_{\mathrm{HH}} & t'_{\mathrm{HV}} \\ r_{\mathrm{VH}} & t'_{\mathrm{VV}} \end{pmatrix} \tag{6.24}$$

holding elements r_{ij} and t'_{ij} of both r and t' respectively. The normalization factor $\mathcal{N}$ given by Eq. (6.14) can be expressed in terms of X using

$$\mathrm{Tr}\,\gamma_1^\dagger\gamma_1 = \mathrm{Tr}\,X^\dagger X - 2\,\mathrm{Per}\,X^\dagger X, \tag{6.25}$$

$$\mathrm{Tr}\,\gamma_2^\dagger\gamma_2 = \mathrm{Tr}\,X^\dagger X - 2\,\mathrm{Det}\,X^\dagger X. \tag{6.26}$$

("Per" denotes the permanent of a matrix.) In the derivation of Eqs. (6.23,6.25,6.26) we have made use of the unitarity of S. The concurrence becomes

$$\mathcal{C} = \frac{2|\alpha|^2\sqrt{\mathrm{Det}\,X^\dagger X\,\mathrm{Det}(\mathbb{1}-X^\dagger X)}}{\mathrm{Tr}\,X^\dagger X-(1+|\alpha|^2)\mathrm{Per}\,X^\dagger X-(1-|\alpha|^2)\mathrm{Det}\,X^\dagger X}. \tag{6.27}$$

Entanglement depends on the amount of temporal indistinguishability $|\alpha|^2$ and the Hermitian matrix

$$X^\dagger X = \begin{pmatrix} |\mathbf{r}_{\mathrm{H}}|^2 & \mathbf{r}_{\mathrm{H}}\cdot\mathbf{t}'_{\mathrm{V}} \\ (\mathbf{r}_{\mathrm{H}}\cdot\mathbf{t}'_{\mathrm{V}})^* & |\mathbf{t}'_{\mathrm{V}}|^2 \end{pmatrix}, \tag{6.28}$$

containing the states $\mathbf{r}_{\rm H} = (r_{\rm HH}, r_{\rm VH})$ and $\mathbf{t}'_{\rm V} = (t'_{\rm HV}, t'_{\rm VV})$ of a reflected and transmitted photon to the left of the beam splitter. The determinant of $X^\dagger X$ measures the size of the span of $\mathbf{r}_{\rm H}$ and $\mathbf{t}'_{\rm V}$ as

$$\mathrm{Det}\, X^\dagger X = |\mathbf{r}_{\rm H}|^2 |\mathbf{t}'_{\rm V}|^2 \left(1 - \frac{|\mathbf{r}_{\rm H}\cdot\mathbf{t}'_{\rm V}|^2}{|\mathbf{r}_{\rm H}|^2|\mathbf{t}'_{\rm V}|^2}\right). \tag{6.29}$$

If $\mathbf{r}_{\rm H}$ and $\mathbf{t}'_{\rm V}$ are parallel ($\mathrm{Det} X^\dagger X = 0$), a scattered photon to the left of the beam splitter is in a definite state, giving rise to an unentangled two-photon state ($\mathcal{C} = 0$). Similarly,

$$\mathrm{Det}(\mathbb{1} - X^\dagger X) = |\mathbf{t}_{\rm H}|^2 |\mathbf{r}'_{\rm V}|^2 \left(1 - \frac{|\mathbf{t}_{\rm H}\cdot\mathbf{r}'_{\rm V}|^2}{|\mathbf{t}_{\rm H}|^2|\mathbf{r}'_{\rm V}|^2}\right) \tag{6.30}$$

involves scattered states $\mathbf{t}_{\rm H} = (t_{\rm HH}, t_{\rm VH})$ and $\mathbf{r}'_{\rm V} = (r'_{\rm HV}, r'_{\rm VV})$ to the right of the beam splitter. The denominator of Eq. (6.27) is the probability of finding a scattered state with one photon on either side of the beam splitter. It deviates from its classical value $(X^\dagger X)_{\rm HH} + (X^\dagger X)_{\rm VV} - 2(X^\dagger X)_{\rm HH}(X^\dagger X)_{\rm VV}$ by an amount $-2|\alpha|^2|(X^\dagger X)_{\rm HV}|^2$ due to photon bunching. This reduction of coincidence count probability is the Mandel dip [17]. It measures the indistinguishability of a reflected and transmitted photon as the product of temporal indistinguishability $|\alpha|^2$ and polarization indistinguishability $|(X^\dagger X)_{\rm HV}|^2$.

6.4 Violation of the Bell-CHSH inequality

The maximal value $\mathcal{E}_{\rm max}$ of the Bell-CHSH parameter (6.8) for an arbitrary mixed state was analyzed in Refs. [18, 19]. For a pure state with concurrence $\mathcal{C}$ one has simply $\mathcal{E}_{\rm max} = 2\sqrt{1+\mathcal{C}^2}$ [20]. For a mixed state there is no one-to-one relation between $\mathcal{C}$ and $\mathcal{E}_{\rm max}$. Depending on the density matrix, $\mathcal{E}_{\rm max}$ can take on values between $2\mathcal{C}\sqrt{2}$ and $2\sqrt{1+\mathcal{C}^2}$. The dependence of $\mathcal{E}_{\rm max}$ on ρ involves the two largest eigenvalues of the real symmetric 3×3 matrix $R^{\rm T}R$ constructed from $R_{kl} = \mathrm{Tr}\,\rho\,\sigma_k \otimes \sigma_l$, where $\sigma_1 = \sigma_x$,$\sigma_2 = \sigma_y$ and $\sigma_3 = \sigma_z$. In terms of γ_1 and γ_2, the elements R_{kl} take the form

$$R_{kl} = \frac{(1+|\alpha|^2)}{\mathcal{N}} \mathrm{Tr}\,\gamma_1^\dagger \sigma_k \gamma_1 \sigma_l^{\rm T} + \frac{(1-|\alpha|^2)}{\mathcal{N}} \mathrm{Tr}\,\gamma_2^\dagger \sigma_k \gamma_2 \sigma_l^{\rm T}. \tag{6.31}$$

The matrix γ_2 has a polar decomposition $\gamma_2 = U\sqrt{\xi}V$ where U and V are unitary matrices and ξ is a diagonal matrix holding the eigenvalues of $\gamma_2^\dagger\gamma_2$. The real positive ξ_i's are determined by

$$\xi_1 + \xi_2 = \mathrm{Tr}\,\gamma_2^\dagger\gamma_2, \quad 2\sqrt{\xi_1\xi_2} = |\mathrm{Tr}\,\gamma_2^\dagger\tilde{\gamma}_2|. \tag{6.32}$$

The matrix γ_1 can be conveniently expressed as (see Appendix 6.B)

$$\gamma_1 = U\,Q\sqrt{\xi}\,V, \quad \text{where} \quad Q = \begin{pmatrix} c_1 & c_2 \\ c_3 & -c_1 \end{pmatrix}. \tag{6.33}$$

The parameters c_1,c_2,c_3 are real numbers. The matrix Q is traceless due to the orthogonality of γ_1 and $\tilde{\gamma}_2$. The number $c_1 \in (-1,1)$ on the diagonal is related to the inner product of γ_1 and γ_2 and takes the form

$$c_1 = \frac{\mathrm{Tr}\,\gamma_1^\dagger \gamma_2}{\xi_1 - \xi_2}, \quad \text{with} \quad \mathrm{Tr}\,\gamma_1^\dagger \gamma_2 = \mathrm{Tr}\,\sigma_z X^\dagger X. \tag{6.34}$$

The numbers c_2,c_3 are determined by the norm and tilde inner product of γ_1 and satisfy the relations

$$c_1^2 + c_2 c_3 = 1, \quad c_1^2(\xi_1+\xi_2) + c_2^2\xi_2 + c_3^2\xi_1 = \mathrm{Tr}\,\gamma_1^\dagger\gamma_1. \tag{6.35}$$

We substitute γ_1 of Eq. (6.33) and the polar decomposition of γ_2 in Eq. (6.31) and parameterize

$$U^\dagger \sigma_k U = \sum_{i=1}^{3} N_{ki}\sigma_i, \quad V\sigma_k^{\mathrm{T}} V^\dagger = \sum_{i=1}^{3} M_{ki}\sigma_i^{\mathrm{T}}, \tag{6.36}$$

in terms of two 3×3 orthogonal matrices N and M. The matrix R takes the form

$$R = N R' M^{\mathrm{T}}, \tag{6.37}$$

where R' is given by Eq. (6.31) with substitutions $R \to R'$, $\gamma_2 \to \sqrt{\xi}$ and $\gamma_1 \to Q\sqrt{\xi}$. With the help of Eqs. (6.32,6.34,6.35), the eigenvalues u_i of $R^{\mathrm{T}}R$ can now be expressed as (see Appendix 6.C)

$$u_1 = \frac{1}{2\mathcal{N}^2}\left(\mathcal{T} + \sqrt{\mathcal{T}^2 - 4\mathcal{D}}\right), \tag{6.38}$$

$$u_2 = \frac{1}{2\mathcal{N}^2}\left(\mathcal{T} - \sqrt{\mathcal{T}^2 - 4\mathcal{D}}\right), \tag{6.39}$$

$$u_3 = 4\frac{|\alpha|^4 |\mathrm{Tr}\,\gamma_1^\dagger \tilde{\gamma}_1|^2}{\mathcal{N}^2}, \tag{6.40}$$

where

$$\mathcal{T} = \mathcal{N}^2 + 4|\mathrm{Tr}\,\gamma_1^\dagger\tilde{\gamma}_1|^2 - 4(1-|\alpha|^4)\left(\mathrm{Tr}\,\gamma_1^\dagger\gamma_1\,\mathrm{Tr}\,\gamma_2^\dagger\gamma_2 - \mathrm{Tr}^2\,\gamma_1^\dagger\gamma_2\right), \tag{6.41}$$

$$\mathcal{D} = 4|\mathrm{Tr}\gamma_1^\dagger\tilde{\gamma}_1|^2\left(\mathcal{N}^2 - 4(1-|\alpha|^4)\mathrm{Tr}\gamma_1^\dagger\gamma_1\mathrm{Tr}\gamma_2^\dagger\gamma_2\right). \tag{6.42}$$

We can relate the u_i's to $X^\dagger X$ and $|\alpha|^2$ using Eqs. (6.14,6.23,6.25,6.26,6.34). The parameter $\mathcal{E}_{\max}$ depends on the two largest eigenvalues of $R^{\mathrm{T}}R$ as

$$\mathcal{E}_{\max} = 2\sqrt{u_1 + \max(u_2, u_3)}. \tag{6.43}$$

Generically, the expression for $\mathcal{E}_{\max}$ takes a complicated form where ordering of u_2 and u_3 depends on $X^\dagger X$ and $|\alpha|^2$.

6.5 Discussion

The objective of the discussion is to reveal the role played by the Mandel dip $-2|\alpha|^2|(X^\dagger X)_{\mathrm{HV}}|^2$ in the connection between $\mathcal{C}$ and $\mathcal{E}_{\max}$.

We first consider the case $|(X^\dagger X)_{\mathrm{HV}}|^2 = 0$. The concurrence of Eq. (6.27) reduces to

$$\mathcal{C} = \frac{2|\alpha|^2\prod_{i=\mathrm{H,V}}\sqrt{(X^\dagger X)_{ii}(1-(X^\dagger X)_{ii})}}{(X^\dagger X)_{\mathrm{HH}} + (X^\dagger X)_{\mathrm{VV}} - 2(X^\dagger X)_{\mathrm{HH}}(X^\dagger X)_{\mathrm{VV}}}. \tag{6.44}$$

The maximal value of the Bell-CHSH parameter takes the form

$$\mathcal{E}_{\max} = 2\sqrt{1+\mathcal{C}^2} \tag{6.45}$$

and $\mathcal{C} > 0$ implies $\mathcal{E}_{\max} > 2$.

In the presence of a Mandel dip ($|\alpha|^2|(X^\dagger X)_{\mathrm{HV}}|^2 > 0$), the ability of $\mathcal{E}$ to witness entanglement can disappear. We consider the special case $(X^\dagger X)_{ii} = 1/2$. This corresponds to $|\mathbf{r}_{\mathrm{H}}|^2 = |\mathbf{t}_{\mathrm{H}}|^2 = 1/2$ and $|\mathbf{r}'_{\mathrm{V}}|^2 = |\mathbf{t}'_{\mathrm{V}}|^2 = 1/2$, which, in particular, is attained if $t^\dagger t = \mathbb{1}/2$. The concurrence of Eq. (6.27) reduces to

$$\mathcal{C} = \frac{|\alpha|^2\left(1-4|(X^\dagger X)_{\mathrm{HV}}|^2\right)}{1-4|\alpha|^2|(X^\dagger X)_{\mathrm{HV}}|^2}. \tag{6.46}$$

To find $\mathcal{E}_{\max}$ we have to consider the ordering of u_2 and u_3 which depends on $|(X^\dagger X)_{\mathrm{HV}}|^2$ and $|\alpha|^2$. The function

$$f(|\alpha|^2) = \frac{|\alpha|^2}{2(1+|\alpha|^2)} \tag{6.47}$$

divides parameter space in the region $|(X^\dagger X)_{\mathrm{HV}}|^2 \leq f$ where $\mathcal{E}_{\max} = 2\sqrt{u_1+u_3}$ and the region $|(X^\dagger X)_{\mathrm{HV}}|^2 > f$ where $\mathcal{E}_{\max} = 2\sqrt{u_1+u_2}$. The equation $\mathcal{E}_{\max} = 2$

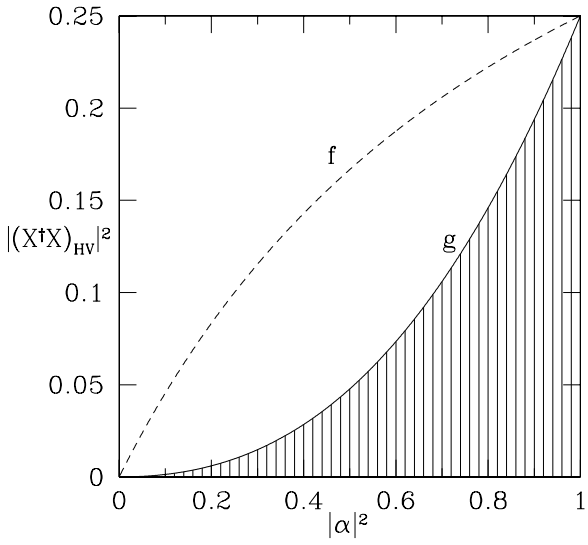

Figure 6.2: Parameter space of a beam splitter with $(X^\dagger X)_{ii} = 1/2$ spanned by $|\alpha|^2 \in (0,1)$ and $|(X^\dagger X)_{\rm HV}|^2 \in (0,1/4)$. All points correspond to a non-vanishing polarization-entanglement ($\mathcal{C} > 0$) except the line segments $|\alpha|^2 = 0$ and $|(X^\dagger X)_{\rm HV}|^2 = 1/4$ where entanglement vanishes ($\mathcal{C} = 0$). Only in the shaded region, the Bell-CHSH parameter is able to detect entanglement ($\mathcal{E}_{\rm max} > 2$). The lines correspond to the functions f, g of Eqs. (6.47,6.48) respectively.

has a solution $g(|\alpha|^2)$ for $|(X^\dagger X)_{\mathrm{HV}}|^2$ that lies in the region $|(X^\dagger X)_{\mathrm{HV}}|^2 \leq f$. The function g takes the form

$$g(|\alpha|^2) = \frac{1}{4}\left(1 - |\alpha|^2 + |\alpha|^4 - (1-|\alpha|^2)\sqrt{1+|\alpha|^4}\right) \tag{6.48}$$

and breaks parameter space in two fundamental regions: a region $|(X^\dagger X)_{\mathrm{HV}}|^2 < g$ where $\mathcal{E}_{\max} > 2$ and a region $|(X^\dagger X)_{\mathrm{HV}}|^2 > g$ where $\mathcal{E}_{\max} < 2$. We have drawn these regions in Fig. 6.2. The maximal value of the Bell-CHSH parameter is given by

$$\mathcal{E}_{\max} = 2\mathcal{C}|\alpha|^{-2}\sqrt{1+|\alpha|^4} \tag{6.49}$$

in the region $|(X^\dagger X)_{\mathrm{HV}}|^2 \leq f$.

6.6 Conclusions

In summary, we have calculated the amount of polarization-entanglement (concurrence $\mathcal{C}$) and its witness (maximal value of the Bell-CHSH parameter $\mathcal{E}$) induced by two-photon interference at a lossless beam splitter. The ability of $\mathcal{E}$ to witness entanglement ($\mathcal{E}_{\max} > 2$) depends on the Mandel dip $-2|\alpha|^2|(X^\dagger X)_{\mathrm{HV}}|^2$. In the absence of a Mandel dip, $\mathcal{C} > 0$ implies $\mathcal{E}_{\max} > 2$ cf. Eq. (6.45), whereas in its presence this is not necessarily true. In the latter case, as we have demonstrated in Sec. 6.5 with $(X^\dagger X)_{ii} = 1/2$, the witnessing ability of $\mathcal{E}$ depends on the individual contributions of temporal ($|\alpha|^2$) and polarization indistinguishability ($|(X^\dagger X)_{\mathrm{HV}}|^2$).

Our results can be applied to interference of other kinds of particles, getting entangled in some $2 \otimes 2$ Hilbert space and being "marked" by an additional degree of freedom. However, determining the indistinguishability parameter $|\alpha|^2$ requires careful analysis of the detection scheme. In case of fermions, the matrices γ_1 and γ_2 of Eq. (6.13) are to be interchanged. Systems without a time-reversal symmetry are captured by the analysis, as we did not make use of the symmetry of the scattering matrix.

6.A arbitrariness of two-photon input state

The unitary scattering matrix has a polar decomposition

$$S = \begin{pmatrix} K' & 0 \\ 0 & L' \end{pmatrix}\begin{pmatrix} \sqrt{\mathbb{1}-T} & i\sqrt{T} \\ i\sqrt{T} & \sqrt{\mathbb{1}-T} \end{pmatrix}\begin{pmatrix} K & 0 \\ 0 & L \end{pmatrix}, \tag{6.50}$$

where K',L',K,L are 2×2 unitary matrices and $T=\mathrm{diag}(T_{\mathrm{H}},T_{\mathrm{V}})$ is a matrix of transmission eigenvalues $T_{\mathrm{H}},T_{\mathrm{V}}\in(0,1)$. The outgoing state $|\Psi_{\mathrm{out}}\rangle$ is related to the 4×4 matrix

$$S\begin{pmatrix}0 & \sigma_{\mathrm{in}}\\ 0 & 0\end{pmatrix}S^{\mathrm{T}} \tag{6.51}$$

cf. Eq. (6.5). By group decomposition $K=K_1K_2$ and $L=L_1L_2$, $|\Psi_{\mathrm{out}}\rangle$ is easily seen to correspond to $K_2\sigma_{\mathrm{in}}L_2^{\mathrm{T}}$ scattered by S of Eq. (6.50) with substitutions $K\to K_1$ and $L\to L_1$.

6.B joint semi-polar decomposition

The matrices γ_1 and γ_2 have a decomposition

$$\gamma_1=U\mathcal{A}V,\quad \gamma_2=U\sqrt{\xi}V, \tag{6.52}$$

where U,V are unitary matrices and ξ is a diagonal matrix of eigenvalues of $\gamma_2^\dagger\gamma_2$. As we do not yet specify $\mathcal{A}$, such a joint decomposition always exists. In our case, the matrices γ_1 and γ_2 have the special properties

$$\mathrm{Tr}\,\gamma_1^\dagger\tilde{\gamma}_1=-\mathrm{Tr}\,\gamma_2^\dagger\tilde{\gamma}_2,\quad \mathrm{Tr}\,\gamma_1^\dagger\tilde{\gamma}_2=0, \tag{6.53}$$

$$|\mathrm{Tr}\,\gamma_1^\dagger\tilde{\gamma}_1|=2\sqrt{\mathrm{Det}\,X^\dagger X\,\mathrm{Det}(\mathbb{1}-X^\dagger X)}, \tag{6.54}$$

$$\mathrm{Tr}\,\gamma_1^\dagger\gamma_1=\mathrm{Tr}\,X^\dagger X-2\,\mathrm{Per}\,X^\dagger X, \tag{6.55}$$

$$\mathrm{Tr}\,\gamma_2^\dagger\gamma_2=\mathrm{Tr}\,X^\dagger X-2\,\mathrm{Det}\,X^\dagger X, \tag{6.56}$$

$$\mathrm{Tr}\,\gamma_1^\dagger\gamma_2=\mathrm{Tr}\,\sigma_z X^\dagger X. \tag{6.57}$$

It is the purpose of this appendix to demonstrate that $\mathcal{A}=Q\sqrt{\xi}$ where Q is a real traceless matrix of Eq. (6.33) with c_1 given by Eq. (6.34) and c_2,c_3 satisfying Eq. (6.35).

The inner and tilde inner product of γ_1 and γ_2 take the form

$$\mathrm{Tr}\,\gamma_1^\dagger\gamma_2=\mathrm{Tr}\,\mathcal{A}^\dagger\sqrt{\xi}, \tag{6.58}$$

$$\mathrm{Tr}\,\gamma_1^\dagger\tilde{\gamma}_2=(\mathrm{Det}\,U\,V)^{-2}\,\mathrm{Tr}\,\mathcal{A}^\dagger\sigma_y\sqrt{\xi}\sigma_y=0. \tag{6.59}$$

(Here we have used the identity $U\sigma_yU^{\mathrm{T}}=\mathrm{Det}^2U\,\sigma_y$, valid for any 2×2 unitary matrix U.) The conditions of Eqs. (6.58,6.59) involve the diagonal elements of $\mathcal{A}$ as respectively

$$\mathrm{Tr}\,\gamma_1^\dagger\gamma_2=\sqrt{\xi_1}\mathcal{A}_{11}^*+\sqrt{\xi_2}\mathcal{A}_{22}^*, \tag{6.60}$$

$$\mathrm{Tr}\,\gamma_1^\dagger\tilde{\gamma}_2 = (\mathrm{Det}\,UV)^{-2}\left(\sqrt{\xi_1}\mathcal{A}_{22}^* + \sqrt{\xi_2}\mathcal{A}_{11}^*\right) = 0. \tag{6.61}$$

It follows that $\mathcal{A}_{11} = c_1^*\sqrt{\xi_1}$ and $\mathcal{A}_{22} = -c_1^*\sqrt{\xi_2}$ where c_1 is given by

$$c_1 = \frac{\mathrm{Tr}\,\gamma_1^\dagger\gamma_2}{\xi_1 - \xi_2}. \tag{6.62}$$

The number c_1 is real since $\mathrm{Tr}\,\gamma_1^\dagger\gamma_2 = \mathrm{Tr}\,\sigma_z X^\dagger X \in \mathbb{R}$.

The determinant of $\mathcal{A}$ is fixed by $\mathrm{Tr}\,\gamma_1^\dagger\tilde{\gamma}_1 = -\mathrm{Tr}\,\gamma_2^\dagger\tilde{\gamma}_2$ implying

$$\mathrm{Det}\,\mathcal{A} = -\sqrt{\xi_1\xi_2}. \tag{6.63}$$

It follows that $\mathcal{A}_{12} = \mathcal{A}'_{12}e^{i\phi}$ and $\mathcal{A}_{21} = \mathcal{A}'_{21}e^{-i\phi}$ with real $\mathcal{A}'_{12}$,$\mathcal{A}'_{21}$,ϕ. The numbers $\mathcal{A}'_{12}$,$\mathcal{A}'_{21}$ satisfy

$$c_1^2\sqrt{\xi_1\xi_2} + \mathcal{A}'_{12}\mathcal{A}'_{21} = \sqrt{\xi_1\xi_2}, \tag{6.64}$$

$$c_1^2(\xi_1+\xi_2) + \mathcal{A}'^2_{12} + \mathcal{A}'^2_{21} = \mathrm{Tr}\,\gamma_1^\dagger\gamma_1, \tag{6.65}$$

where Eq. (6.65) comes from $\mathrm{Tr}\,\mathcal{A}^\dagger\mathcal{A} = \mathrm{Tr}\,\gamma_1^\dagger\gamma_1$. The undetermined phase ϕ can be taken out,

$$\mathcal{A} = \begin{pmatrix} e^{i\frac{\phi}{2}} & 0 \\ 0 & e^{-i\frac{\phi}{2}} \end{pmatrix}\begin{pmatrix} \mathcal{A}_{11} & \mathcal{A}'_{12} \\ \mathcal{A}'_{21} & \mathcal{A}_{22} \end{pmatrix}\begin{pmatrix} e^{-i\frac{\phi}{2}} & 0 \\ 0 & e^{i\frac{\phi}{2}} \end{pmatrix}, \tag{6.66}$$

and absorbed in the unitary matrices U and V by the transformations

$$U\begin{pmatrix} e^{i\frac{\phi}{2}} & 0 \\ 0 & e^{-i\frac{\phi}{2}} \end{pmatrix} \to U, \quad \begin{pmatrix} e^{-i\frac{\phi}{2}} & 0 \\ 0 & e^{i\frac{\phi}{2}} \end{pmatrix}V \to V. \tag{6.67}$$

(Note that these transformations also hold for γ_2 since $\sqrt{\xi}$ commutes with a diagonal matrix of phase factors.)

The matrix $\mathcal{A}$ is related to Q by $\mathcal{A} = Q\sqrt{\xi}$. It is now easily seen that the matrix Q is real and traceless and takes the form of Eq. (6.33), with c_1 given by Eq. (6.34) and c_2,c_3 satisfying Eq. (6.35).

As a last step we perform a consistency check to demonstrate that Eqs. (6.64) and (6.65) have solutions for $\mathcal{A}'_{12}$ and $\mathcal{A}'_{21}$. The Hermitian matrix $X^\dagger X$ has an eigenvalue-eigenvector decomposition

$$X^\dagger X = W^\dagger\Lambda W. \tag{6.68}$$

In terms of the eigenvalues $\Lambda_i \in (0,1)$ and the unitary matrix W, the inner product of γ_1 and γ_2 and the ξ_i's take the form

$$\mathrm{Tr}\,\gamma_1^\dagger\gamma_2 = \Lambda_1(|W_{11}|^2 - |W_{12}|^2) + \Lambda_2(|W_{21}|^2 - |W_{22}|^2), \tag{6.69}$$

$$\xi_1 = \Lambda_1(1-\Lambda_2), \quad \xi_2 = \Lambda_2(1-\Lambda_1). \tag{6.70}$$

It follows that $c_1 = \cos 2\eta$, where we have set $|W_{11}| = |W_{22}| = \cos\eta$ and $|W_{12}| = |W_{21}| = \sin\eta$. Eqs. (6.64,6.65) can be expressed as respectively

$$\mathcal{A}'_{12}\mathcal{A}'_{21} = \sin^2 2\eta \sqrt{\Lambda_1\Lambda_2(1-\Lambda_1)(1-\Lambda_2)}, \tag{6.71}$$

$$\mathcal{A}'^2_{12} + \mathcal{A}'^2_{21} = \sin^2 2\eta\,(\Lambda_1(1-\Lambda_1) + \Lambda_2(1-\Lambda_2)). \tag{6.72}$$

Since

$$2\sqrt{\Lambda_1\Lambda_2(1-\Lambda_1)(1-\Lambda_2)} \leq \Lambda_1(1-\Lambda_1) + \Lambda_2(1-\Lambda_2) \tag{6.73}$$

a family of solutions exists.

6.C eigenvalues of $\mathbf{R^T R}$

The non-vanishing elements of R' are given by

$$R'_{11} = \frac{2}{\mathcal{N}}\left(1-|\alpha|^2-(1+|\alpha|^2)(c_1^2-c_2c_3)\right)\sqrt{\xi_1\xi_2}, \tag{6.74}$$

$$R'_{13} = \frac{2}{\mathcal{N}}(1+|\alpha|^2)c_1(c_2\xi_2+c_3\xi_1), \tag{6.75}$$

$$R'_{22} = \frac{2}{\mathcal{N}}\left(-1+|\alpha|^2+(1+|\alpha|^2)(c_1^2+c_2c_3)\right)\sqrt{\xi_1\xi_2}, \tag{6.76}$$

$$R'_{31} = \frac{2}{\mathcal{N}}(1+|\alpha|^2)c_1(c_2+c_3)\sqrt{\xi_1\xi_2}, \tag{6.77}$$

$$R'_{33} = \frac{1}{\mathcal{N}}\left((1-|\alpha|^2)+(1+|\alpha|^2)c_1^2\right)(\xi_1+\xi_2) \tag{6.78}$$

$$-\frac{1}{\mathcal{N}}(1+|\alpha|^2)(c_2^2\xi_2+c_3^2\xi_1). \tag{6.79}$$

The matrix $R'^{\mathrm{T}}R'$ has eigenvalues

$$u_1 = \frac{1}{2\mathcal{N}^2}\left(\mathcal{T}+\sqrt{\mathcal{T}^2-4\mathcal{D}}\right), \tag{6.80}$$

$$u_2 = \frac{1}{2\mathcal{N}^2}\left(\mathcal{T}-\sqrt{\mathcal{T}^2-4\mathcal{D}}\right), \tag{6.81}$$

$$u_3 = R'^2_{22}, \tag{6.82}$$

where $\mathcal{T}$,$\mathcal{D}$ are the trace, determinant respectively of the 2×2 real symmetric matrix

$$\mathcal{N}^2 \begin{pmatrix} R'^2_{11} + R'^2_{31} & R'_{11}R'_{13} + R'_{31}R'_{33} \\ R'_{11}R'_{13} + R'_{31}R'_{33} & R'^2_{13} + R'^2_{33} \end{pmatrix}. \tag{6.83}$$

By making use of Eqs. (6.34,6.35) u_3,$\mathcal{T}$,$\mathcal{D}$ can be simplified to yield the results of Eqs. (6.40,6.41,6.42) respectively.

Bibliography

[1] B. Yurke and D. Stoler, Phys. Rev. Lett. **68**, 1251 (1992); Phys. Rev. A **46**, 2229 (1992).

[2] Y. H. Shih and C. O. Alley, Phys. Rev. Lett. **61**, 2921 (1988).

[3] Z. Y. Ou and L. Mandel, Phys. Rev. Lett. **61**, 50 (1988).

[4] T. B. Pittman and J. D. Franson, Phys. Rev. Lett. **90**, 240401 (2003).

[5] D. Fattal, K. Inoue, J. Vučković, C. Santori, G. S. Solomon, and Y. Yamamoto, Phys. Rev. Lett. **92**, 037903 (2004).

[6] M. Żukowski, A. Zeilinger, M. A. Horne, and A. K. Ekert, Phys. Rev. Lett. **71**, 4287 (1993).

[7] J. -W. Pan, D. Bouwmeester, H. Weinfurter, and A. Zeilinger, Phys. Rev. Lett. **80**, 3891 (1998).

[8] J. -W. Pan, M. Daniell, S. Gasparoni, G. Weihs, and A. Zeilinger, Phys. Rev. Lett. **86**, 4435 (2001).

[9] T. Jennewein, G. Weihs, J. -W. Pan, and A. Zeilinger, Phys. Rev. Lett. **88**, 017903 (2002).

[10] E. Knill, R. Laflamme, and G. J. Milburn, Nature **409**, 46 (2001).

[11] J. D. Franson, M. M. Donegan, M. J. Fitch, B. C. Jacobs, and T. B. Pittman, Phys. Rev. Lett. **89**, 137901 (2002).

[12] R. P. Feynman, *Lectures on Physics* (Addison-Wesley, 1969), Vol. 3.

[13] S. Bose and D. Home, Phys. Rev. Lett. **88**, 050401 (2002).

[14] R. J. Glauber, Phys. Rev. **130**, 2529 (1963); Phys. Rev. **131**, 2766 (1963).

[15] J. F. Clauser, M. A. Horne, A. Shimony, and R. A. Holt, Phys. Rev. Lett. **23**, 880 (1969).

[16] W. K. Wootters, Phys. Rev. Lett. **80**, 2245 (1998).

[17] C. K. Hong, Z. Y. Ou, and L. Mandel, Phys. Rev. Lett. **59**, 2044 (1987).

[18] R. Horodecki, P. Horodecki, and M. Horodecki, Phys. Lett. A **200**, 340 (1995).

[19] F. Verstraete and M. M. Wolf, Phys. Rev. Lett. **89**, 170401 (2002).

[20] N. Gisin, Phys. Lett. A **154**, 201 (1991).

Samenvatting

Verstrengeling (in het Engels “entanglement”) is een quantummechanische correlatie tussen twee ruimtelijk gescheiden deeltjes. Voor elektronen is de correlatie over het algemeen tussen spintoestanden, voor fotonen tussen polarisaties. Zo’n quantummechanische correlatie is veel sterker dan kan worden verklaard met de klassieke mechanica. Verstrengeling is niet alleen een wonderlijk verschijnsel, het is ook nuttig: verstrengelde deeltjes zijn de “brandstof” voor een quantumcomputer.

Verstrengeling is experimenteel aangetoond voor fotonen in de vrije ruimte, maar nog niet voor elektronen in de vaste stof. In dit proefschrift stellen we een verrassend eenvoudige methode voor om mobiele ladingsdragers in een geleider te verstrengelen. Ook geven we aan hoe deze verstrengeling kan worden gemeten in het laboratorium. De methode is zo eenvoudig, omdat er, in tegenstelling tot eerdere voorstellen, geen wisselwerking tussen de elektronen nodig is. De methode kan gerealiseerd worden in twee-dimensionale elektronengassen in hoog magnetisch veld, zoals experimenteel onderzocht in Delft.

De verstrengeling is tussen spintoestanden van een elektron en een gat, ruimtelijk gescheiden door een tunnelbarrière. Elektron-gat paren ontstaan door een spanningsverschil aan te leggen over de barrière. Het optisch analogon is een bundelsplitser uit de lineaire optica. In tegenstelling tot de bundelsplitser, die geen fotonen kan verstrengelen afkomstig van een thermische bron (zoals een gloeilamp), werkt de tunnelbarrière wel voor elektronen in thermisch evenwicht. Een ander verschil tussen de elektronische en optische verstrengeling is dat in het elektronische geval geen synchronisatie nodig is: elektron-gat paren ontstaan automatisch op hetzelfde moment, terwijl in het optische geval twee fotonen de bundelsplitser gelijktijdig moeten bereiken.

Verstrengeling is kwetsbaar: de quantummechanische correlatie gaat gemakkelijk verloren door wisselwerking met de omgeving. In dit proefschrift onderzoeken we zowel elastische wisselwerking als inelastische wisselwerking (decoherentie). Verstrengeling blijkt opvallend robuust met betrekking tot elastische

wisselwerking, in overeenkomst met een optisch experiment uitgevoerd in Leiden.

De opbouw van dit proefschrift is als volgt. Hoofdstuk 1 is een korte inleiding met achtergrondinformatie over verstrengeling. De hoofdstukken 2 en 3 gaan over elektron-gat verstrengeling, waarbij de produktie van verstrengeling wordt behandeld in hoofdstuk 2 en de invloed van decoherentie in hoofdstuk 3. In de hoofdstukken 4, 5 en 6 richten we ons op fotonen. De hoofdstukken 4 en 5 gaan over elastische wisselwerking van twee verstrengelde fotonen met hun omgeving. Hoofdstuk 6, ten slotte, gaat over de produktie van verstrengeling met een bundelsplitser. We berekenen de relatie tussen de synchronisatie van twee fotonen en de verstrengeling van hun polarisaties aan de bundelsplitser.

List of publications

- *Ab initio thermodynamics of bcc- and fcc cesium*, N. E. Christensen, D. J. Boers, J. L. van Velsen, and D. L. Novikov, Journal of Physics: Condensed Matter **12**, 3293 (2000).
- *Negative thermal expansion coefficient and isostructural transition in fcc cesium*, N. E. Christensen, D. J. Boers, J. L. van Velsen, and D. L. Novikov, Physical Review B **61**, 3764 (2000).
- *Ab initio thermodynamics of bcc- and fcc cesium*, N. E. Christensen, D. L. Novikov, D. J. Boers, and J. L. van Velsen, Bulletin of the American Physical Society **45**, 56 (2000).
- *Scattering theory of plasmon-assisted entanglement transfer and distillation*, J. L. van Velsen, J. Tworzydło, and C. W. J. Beenakker, Physical Review A **68**, 043807 (2003). [chapter 4]
- *Proposal for production and detection of entangled electron-hole pairs in a degenerate electron gas*, C. W. J. Beenakker, C. Emary, M. Kindermann, and J. L. van Velsen, Physical Review Letters **91**, 147901 (2003). [chapter 2]
- *Dephasing of entangled electron-hole pairs in a degenerate electron gas*, J. L. van Velsen, M. Kindermann, and C. W. J. Beenakker, Turkish Journal of Physics **27**, 323 (2003). [chapter 3]
- *Transition from pure-state to mixed-state entanglement by random scattering*, J. L. van Velsen and C. W. J. Beenakker, Physical Review A **70**, 032325 (2004). [chapter 5]
- *Entangling ability of a beam splitter in the presence of temporal which-path information*, J. L. van Velsen, Physical Review A **72**, 012334 (2005). [chapter 6]

Curriculum Vitæ

Ik ben geboren op 27 juli 1977 te Wageningen. Vanaf 1989 tot 1995 heb ik middelbaar onderwijs gevolgd op het Wagenings Lyceum te Wageningen, afgesloten met het VWO diploma.

Vervolgens begon ik aan de studie natuurkunde aan de Universiteit Twente. De lente en zomer van 1999 heb ik doorgebracht aan de Universiteit van Aarhus in Denemarken. Daar deed ik theoretisch werk in de groep van Prof. dr. N. E. Christensen. Dit werk behelsde ab initio berekeningen van thermodynamische eigenschappen van cesium onder hoge druk. Mijn afstudeeronderzoek deed ik in de periode 2000-2001 in de groep van Prof. dr. N. F. van Hulst. De titel van mijn scriptie is "Theoretical analysis of collective radiation properties of identical molecules with arbitrary orientations". Het doctoraal examen (cum laude) behaalde ik in 2001. Gedurende mijn studie ben ik studentassistent geweest bij het Natuurkundig Practicum. Tevens bezocht ik een zomerschool in Oxford (Engeland), met steun van de faculteit Technische Natuurkunde van de Universiteit Twente.

In januari 2002 begon ik mijn promotieonderzoek aan de Universiteit Leiden in dienst van de Stichting voor Fundamenteel Onderzoek der Materie (FOM). Ik werkte op het Instituut-Lorentz van het Leids Instituut voor Onderzoek in de Natuurkunde onder begeleiding van Prof. dr. C. W. J. Beenakker aan het onderzoek beschreven in dit proefschrift. Naast mijn onderzoek assisteerde ik bij het college Elektromagnetisme II. Tevens volgde ik zomerscholen in Hakone (Japan), Istanbul (Turkije), Wittenberg (Duitsland) en Nijmegen en presenteerde mijn werk op conferenties in Orlando (Verenigde Staten) en Enschede.

Stellingen

behorend bij het proefschrift

On the production and transfer of entangled electrons and photons

1. The optical no-go theorem of Xiang-bin [*Phys. Rev. A* **66**, *024303 (2002)*] does not extend to the electronic case.

   This thesis, chapter 2.

2. Plasmon-assisted entanglement transfer may reduce as well as increase the degree of entanglement of the photon pairs.

   This thesis, chapter 4.

3. The polarization-entanglement of two photons scattered separately by disorder decays exponentially with the number of detected modes if the scattering mixes polarizations and algebraically if it does not.

   This thesis, chapter 5.

4. In the presence of a Mandel dip, a test of the Bell-CHSH inequality by coincidence detection may fail to reveal the polarization-entanglement induced by a beam splitter.

   This thesis, chapter 6.

5. The entanglement of electron-hole pairs produced by application of a voltage V over a tunnel barrier vanishes identically for temperatures in excess of a critical temperature of order eV/k_BT.

6. A two-dimensional electron gas with spin-orbit coupling supports spin-polarized edge channels in zero magnetic field.

7. In a certain pressure range, the thermal expansion coefficient of fcc cesium is negative for all temperatures.

   N. E. Christensen, D. J. Boers, J. L. van Velsen, and D. L. Novikov, Phys. Rev. B **61**, *3764 (2000).*

8. The long-wavelength approximation in quantum optics may blur your view too drastically.

Joris van Velsen
28 September 2005